Glutamate neurotransmission from leptin receptor cells is required for typical puberty and reproductive function in female mice

Cristina Sáenz de Miera[1], Nicole Bellefontaine[1], Susan J. Allen[1], Martin G. Myers[1,2,3] Jr., Carol F. Elias[1,2,4]

[1]Department of Molecular and Integrative Physiology; [2]Elizabeth W. Caswell Diabetes Institute; [3]Department of Internal Medicine, Division of Metabolism, Endocrinology and Diabetes, [4]Department of Obstetrics and Gynecology; University of Michigan, Ann Arbor, MI, 48109-5622, USA

Short title: PMv LepRb role in reproduction requires glutamate

Corresponding Author:

Carol F. Elias, PhD
2800 N Plymouth Rd,
North Campus Research Complex, B25-3682
Ann Arbor - MI 48109-5622, USA
Phone: +1 (734) 647-3875
Email: cfelias@umich.edu

Number of pages: 43

Number of figures: 7

Number of tables: 3

Number of words for abstract: 258

Number of words in main text: 4606

ABSTRACT

The hypothalamic ventral premammillary nucleus (PMv) is a glutamatergic nucleus essential for the metabolic control of reproduction. However, conditional deletion of leptin receptor (LepRb) in vesicular glutamate transporter 2 (Vglut2) expressing neurons results in virtually no reproductive deficits. In this study, we determine the role of glutamatergic signaling from leptin responsive PMv neurons on puberty and fertility. We first assessed if stimulation of PMv neurons induces LH release in fed adult females. We used the stimulatory form of designer receptor exclusively activated by designer drugs (DREADDs) in LepRb-Cre mice. We collected blood sequentially before and for 1h after iv. clozapine-N-oxide injection. LH level increased in animals correctly targeted to the PMv, and LH level was correlated to the number of cFos immunoreactive neurons in the PMv. Next, females with deletion of *Vglut2* in LepRb neurons ($LepR^{\Delta VGlut2}$) showed delayed age of puberty, disrupted estrous cycles, increased GnRH concentration in the axon terminals and disrupted LH responses, suggesting impaired GnRH release. To assess if glutamate is required for PMv actions in pubertal development, we generated a Cre-induced reexpression of endogenous LepRb ($LepR^{loxTB}$) with concomitant deletion of Vglut2 (*Vglut2*-floxed) mice. Rescue of Lepr and deletion of Vglut2 in the PMv was obtained by stereotaxic injection of an adeno-associated virus vector expressing Cre recombinase. Control $LepR^{loxTB}$ mice with PMv LepRb rescue showed vaginal opening, follicle maturation and became pregnant, while $LepR^{loxTB}$;$Vglut2^{flox}$ mice showed no pubertal development. Our results indicate that glutamatergic signaling from leptin sensitive neurons regulates the reproductive axis, and that leptin action on pubertal development via PMv neurons requires Vglut2.

SIGNIFICANCE STATEMENT

Age of puberty and reproductive function are strongly influenced by energy balance. Leptin is the primary metabolic hormone in reproductive control, but the neural circuitry involved is not fully understood. Previous studies have suggested that GABAergic but not glutamatergic neurotransmission is required for leptin action on reproduction. However, the PMv, a nucleus essential for the metabolic control of the reproductive function, densely expresses *Lepr* and is essentially glutamatergic. Here we show that remote activation of leptin-responsive neurons in the PMv induces LH secretion, while deletion of glutamatergic neurotransmission in LepR (or PMv) neurons disrupts pubertal development and impairs the reproductive function in female mice. Our findings indicate that glutamate in LepR, and specifically in PMv, neurons is required for reproductive maturation and function.

INTRODUCTION

Reproduction is strongly influenced by nutritional status due to the high energy demand required for this function. Food scarcity leads to suppression of fertility (Ahima et al., 1996; Bronson and Marsteller, 1985; Cagampang et al., 1990; Cameron et al., 1991; Parfitt et al., 1991). Similarly, excess adiposity may induce ovulatory dysfunctions, higher risks of pregnancy complications and earlier age at puberty onset (Biro et al., 2006; Burt Solorzano and McCartney, 2010; Mahany et al., 2018). Metabolic cues signal energy status to the hypothalamo-pituitary-gonadal (HPG) axis, but the sites of action and mechanisms are not fully elucidated.

The adipocyte-derived hormone leptin is an essential metabolic signal acting in the brain to regulate the reproductive axis. Mice and humans with mutations in the leptin or leptin receptor genes are infertile and remain in a prepubertal state (Bray and York, 1979; Farooqi et al., 2007, 2002). Specific restoration of the leptin receptor (*Lepr)* gene only in neurons of *Lepr* deficient mice rescues infertility (De Luca et al., 2005; Quennell et al., 2009). It is well accepted that leptin action in the modulation of the HPG axis is indirect. Gonadotropin-releasing hormone (GnRH) neurons do not express LepR (Quennell et al., 2009) but they do receive direct innervation from *Lepr* expressing neurons (Louis et al., 2011). The neural circuitry involved, however, is incompletely known.

An often-overlooked hypothalamic site, rich in neurons expressing the long form of LepR (LepRb), is the ventral premammillary nucleus (PMv) (Donato et al., 2011; Han et al., 2020; Leshan et al., 2009; Louis et al., 2011; Ross et al., 2018; Scott et al., 2009). In rats, bilateral lesions of the PMv disrupt estrous cycles and the ability of leptin to increase luteinizing hormone (LH) secretion following a fast (Donato et al., 2009). Endogenous restoration of LepRb exclusively in PMv neurons rescues pubertal maturation and fertility in LepR-null female mice (Donato et al., 2011).

Leptin responsive neurons in the PMv project directly to and make contacts with GnRH cell bodies and their terminals in the adjacencies of the median eminence (Boehm et al., 2005; Canteras et al., 1992; Donato et al., 2011; Leshan et al., 2009). These cells also project to the anteroventral periventricular (AVPV) and arcuate (Arc) nuclei, home of kisspeptin (*Kiss1* gene) neurons, the main GnRH regulatory population (Canteras et al., 1992; Donato et al., 2011).

Projections from the PMv make apparent contacts with *Kiss1* expressing cells in the AVPV (Donato et al., 2011), and stimulation of PMv neurons directly activates kisspeptin cells in both the AVPV and the Arc (Ross et al., 2018).

The PMv is essentially glutamatergic (Vong et al., 2011). LepRb neurons coexpress the vesicular glutamate transporter (Vglut2) (Donato et al., 2011), and acute administration of leptin depolarizes most of these neurons (Williams et al., 2011). Glutamatergic terminals are abundant in GnRH (Moore et al., 2018; Yeo et al., 2021) and in kisspeptin (Porter et al., 2021) neurons, while states of low leptin levels, as in fasting, reduce the number of glutamatergic synaptic inputs to kisspeptin neurons of male macaques (Shamas et al., 2015). Prior data, however, has shown that congenital deletion of *Lepr* in glutamatergic neurons has virtually no effect on pubertal development or reproductive function (Martin et al., 2014; Zuure et al., 2013).

In the attempt to untangle these apparent inconsistencies, we used chemogenetics to determine if remote stimulation of PMv neurons induces LH release in diestrous mice. We next used several transgenic mouse models to determine whether disruption of glutamate signaling from *Lepr* neurons impairs leptin-induced puberty and normal reproductive function. Overall, our results indicate that glutamatergic signaling from leptin responsive PMv neurons is required for normal reproductive development and function.

RESULTS

Chemogenetic activation of LepRb-Cre cells in the PMv induces LH secretion

To examine if activation of PMv LepRb neurons induces LH release in fed adult mice, we stereotaxically injected an adeno-associated virus vector (AAV) carrying the stimulatory form of designer receptor exclusively activated by designer drugs (DREADDs), hM3Dq, fused to mCherry (AAV-hM3Dq) unilaterally into the PMv of LepRb-Cre mice, followed by intravenous (iv.) injection of clozapine-N-oxide (CNO) or its metabolite, clozapine, after 4 weeks. Successful infection was confirmed by localized expression of mCherry and cFos immunoreactivity (ir) in the PMv following CNO or clozapine injection. For clarification, Table 1 shows the different experimental, positive and negative control groups, according to AAV and drug delivered, injection site and LH response.

From the AAV-hM3Dq animals that received CNO, 15 out of 18 LepRb-Cre diestrous females had successful AAV-hM3Dq injections (mCherry- and cFos-ir) in the PMv and were considered "PMv-hits" (Fig 1A-B). Two mice showed injections outside the PMv (n=2) and were considered "PMv-misses". The remaining mouse had a very small injection in the PMv (few mCherry-ir neurons, but no cFos-ir) and was removed from the analysis (Table 1). An additional group of 5 mice was injected with an AAV-mCherry vector and received iv. CNO, serving as negative controls. All 5 mice showed successful viral target in the PMv. For representation, this group is shown together with the PMv-misses as "negative controls" (Table 1). An additional group of 4 mice carrying the AAV-hM3Dq received instead iv. clozapine to test the effect of the CNO metabolite. All 4 females showed successful viral target and cFos-ir in PMv neurons, and minimal cFos-ir in other hypothalamic sites (Table 1, Figure 2A-B). An additional negative control group (n=7) did not receive an AAV injection and was injected with clozapine, to evaluate the effect of clozapine alone on LH release (Table 1).

About 55% (8/15) of mice with unilateral AAV-hM3Dq centered in the PMv showed an increase in LH release above 0.5ng/ml within 10-20 min following the CNO injection (0.65-3.11 ng/mL). The remaining PMv-hit animals showed no increase in LH levels following the CNO injection. In PMv-miss animals, a modest increase in LH was observed in one animal (0.57 ng/mL) 10 min after the CNO injection and no increase was observed (under limit of detection) in the other. Only one of the 5 AAV-mCherry injected animals showed an increase in LH (0.93 ng/mL), but it was at 30 min following the iv injection (Fig 1C-D).

The area under the curve (AUC) was calculated for LH levels between 10 minutes before (-10) the injection until 20 minutes after the injection (time 0 was omitted since a few of the animals missed this sampling point) for all the groups, considering the point -10 min as baseline 0. The positive AUC for the PMv-hit with LH increase group was significantly different from 0, indicating a significant rise in LH levels during this time period, while the positive AUC in the other groups did not differ from 0 indicating that LH did not increase following the injection (Fig 1E, F).

The number of cFos-ir neurons per section in the PMv was variable between groups, with higher number of cFos-ir neurons observed in PMv-hits that showed increased LH, than in animals that showed no LH increase and in negative controls (PMv-misses and AAV-mCherry combined)

(Fig 1G). Peak LH levels (ng/mL) were positively correlated to the number of cFos-ir neurons in the PMv, suggesting a link between stimulation of LepRb neurons in the PMv and induction of LH release (Fig 1H). It also suggests that there is a threshold in which a number or a subset of PMv LepRb is necessary for successful stimulation of LH secretion.

All mice with AAV-hM3Dq targeting the PMv (cFos-ir) and injected with clozapine also showed an increase in LH 10 min after the injection (0.87-1.18ng/ml, Fig 2A, B), whereas 2 out of 7 (29%) control mice with no AAV showed an increase in LH following the clozapine injection (Fig 2C). The positive AUC between -10 to 20 min showed a significant increase in LH levels in the Clozapine AAV-hM3Dq group, but not in the group with no AAV (Fig 2D, E). The number of cFos-ir neurons per section in the PMv was higher in animals with hM3Dq than in those with no AAV, in which almost no cFos-ir cells were observed (Fig 2F). Whether this variability in the control animals is due to spontaneous LH release (Czieselsky et al., 2016) needs further investigation.

AAV-hM3Dq contamination of the posterior Arc produces inconsistent CNO-stimulated LH secretion

As expected, the PMv-hit group showed some variability in the injection size, often contaminating to different extent LepRb neurons in areas adjacent to the PMv, including the posterior region of the Arc. Because this region has several neuronal populations involved in the control of reproduction, we evaluated the number of cFos-ir neurons in the Arc that coexpressed mCherry to assess if Arc neuronal activation was either direct or secondary to PMv neuronal activation (Ross et al., 2018). The total number of neurons coexpressing both cFos- and mCherry-ir per section in the posterior Arc was higher in PMv-hit animals, whether or not they showed an increase in LH, than in negative control animals (PMv-miss and AAV-mCherry combined) (Fig 3A-D). As observed for the PMv, peak LH levels were positively correlated to the number of cFos-ir + mCherry-ir neurons in the Arc (Fig 3D), but not with the total number of cFos-ir neurons alone in the Arc ($r=0.3$; $p=0.16$). This observation suggested that LepR expressing neurons in the Arc may have contributed to the increase in LH observed following CNO treatment.

Within the Arc, POMC neurons coexpress LepR and have been shown to stimulate the reproductive axis (Manfredi-Lozano et al., 2016). To understand if direct activation of these neurons could have played a role in the induction of LH, we evaluated the percentage of activated neurons that expressed POMC peptide and the extent of mCherry colocalization in Fos-ir POMC neurons in PMv-Hit group with higher contamination of the Arc, that also had some of the highest LH peaks, and in 3 hM3Dq clozapine animals with elevated LH levels but low mCherry contamination in the Arc. Coexpression of POMC-ir was observed in 9.3 ± 2.6 % (12.3 ± 5.0 neurons) of the cFos-ir neurons of the posterior Arc in the PMv-Hit animals and 9.6 ± 3.1 % (2.3 ± 1.3 neurons) in the hM3Dq clozapine animals. Of these POMC-/cFos-ir neurons, about 50% also coexpressed mCherry-ir (7.3 ± 3.2 neurons) in the PMv-Hit animals, but almost none in the hM3Dq clozapine animals (0.3 ± 0.3 neurons, Fig 3E-G). The small number of mCherry/cFos-ir neurons suggests that contamination of POMC neurons may have only mild (if any) contribution to the higher increases in LH observed in some animals, but it is not determinant for inducing LH release.

We and others have previously shown that only about 10% of Arc Kiss1 (KNDy) neurons of female mice coexpress LepR (Cravo et al., 2013; Donato et al., 2011; Louis et al., 2011; True et al., 2011). To assess if contamination of KNDy neurons could have contributed to the induction of LH, we used LepRb-Cre; Kiss1-hrGFP mouse model to access the expression of cFos-ir and/or mCherry-ir in KNDy neurons following AAV-hM3Dq injections in the PMv (n=4 PMv-hits, Fig 1C). In these animals, only 2.5 ± 0.95 % of cFos-ir neurons in the posterior Arc were also Kiss1-hrGFP positive (1.8 ± 0.3 neurons), and most of these expressed mCherry, suggesting that 1 or 2 KNDy neurons were directly activated by the virus. The low numbers of KNDy neurons expressing cFos-ir in Kiss1-hrGFP PMv-hit mice indicates the increase in LH does not require KNDy neuronal activation (Fig 3H-J) in agreement with previous studies from our group showing that direct leptin action in Kiss1 neurons is neither required nor sufficient for puberty and reproduction (Cravo et al., 2013).

Glutamate neurotransmission in LepRb cells is necessary for typical pubertal timing and estrous cycles

As most of LepRb PMv neurons are glutamatergic (Donato et al., 2011; Zuure et al., 2013) we generated mice that lack Vglut2 in LepRb neurons (LepRb$^{\Delta Vglut2}$) to assess whether glutamatergic neurotransmission from LepRb cells is necessary for reproductive function.

As observed in (Tong et al., 2007), virtually no *Vglut2* expression was noticed in *Lepr* neurons of LepRb$^{\Delta Vglut2}$ mice (Fig 4A-D). Adult LepRb$^{\Delta Vglut2}$ mice (13-26 weeks old) developed late onset obesity (Fig 4E-F) due to increased fat mass in both sexes (Fig 4G-H), reproducing the metabolic phenotype described before for these animals (Xu et al., 2013).

We then assessed if the lack of Vglut2 in LepRb cells alters pubertal maturation and adult reproduction. A thorough assessment of the metabolic and reproductive phenotype of the LepRb-Cre mouse was performed before (García-Galiano et al., 2017), and we found that they are indistinguishable from littermates negative for Cre. Female LepRb$^{\Delta Vglut2}$ and control LepRb-Cre littermates had similar age of vaginal opening and showed no differences in body weight at puberty onset (Fig 5A, B). The day of first estrus, however, was delayed in LepRb$^{\Delta Vglut2}$ mice (Fig 5C). Of note, no differences in body weight were observed at vaginal opening (puberty onset) and first estrus (puberty completion) between experimental and control groups (Fig 5D). In males, balanopreputial separation (BPS) was monitored from P25 as a sign of puberty completion. No differences in age at BPS were found between LepRb-Cre and LepRb$^{\Delta Vglut2}$ littermates (Fig 5E). LepRb$^{\Delta Vglut2}$ male mice showed larger body weight than LepRb-Cre mice at the time of BPS (Fig 5F).

Length of estrous cycles was longer (10-16 weeks of age, before difference in body weight, Fig 5G-I) and the number of cycles completed in 30 days was lower in LepRb$^{\Delta Vglut2}$ mice compared to controls (LepRb-Cre: 4.47 ± 0.30 cycles; LepRb$^{\Delta Vglut2}$: 3.31 ± 0.36 cycles; t_{26} = 2.45; p=0.021). Female LepRb$^{\Delta vglut2}$ spent similar time in estrus, less time in proestrus and more time in diestrus (Fig 5J). Analysis of female fertility showed that 75% of LepRb$^{\Delta Vglut2}$ against 100% of control mice produced at least one litter for 60 days since mating. Comparing fertile females, no differences were observed in latency to pregnancy (Fig 5K) or in the number of pups in the first litter (LepRb-Cre: 7.86 ± 1.14 pups; LepRb$^{\Delta Vglut2}$: 7.50 ± 1.41 pups; t_{11} = 0.20; p=0.85).

Because delay in first estrus, disruption of the estrous cycles and mild subfertility were observed before differences in body weight appeared (arrow in Fig 4B), our findings indicate that the

disruption in reproductive function is caused by deficient glutamatergic neurotransmission in LepRb cells, not by metabolic dysregulation.

To gain insights into the underlying mechanisms associated with the disrupted reproductive function, we evaluated the HPG function. LepRb$^{\Delta Vglut2}$ females had denser GnRH-ir fibers in the Arc than Vglut2^{flox} control females (Fig 6A-C) suggesting retention of the neuropeptide at the neuronal terminals. To assess basal and stimulated GnRH release we measured basal LH and LH in response to intraperitoneal (ip.) injection of kisspeptin. Basal LH levels of diestrous females were not different between genotypes (Fig 6D). An immediate increase in LH (7 minutes) was observed following ip. kisspeptin in both groups, but LH levels in LepRb$^{\Delta Vglut2}$ mice was about half those observed in the controls (Fig 6E). Similarly, the overall LH AUC for the 30-minute period following the kisspeptin-10 injection in LepRb$^{\Delta Vglut2}$ females was about half the area observed in the controls (Fig 6F). These results suggest a deficit in GnRH release despite higher accumulation of peptide at the terminals, which may be due to decreased pituitary LH content or disruption of hypothalamic regulation of GnRH release.

Pituitary expression of *GnRHr*, *LHβ*, *FSHβ* (Fig 6G-I) and the common glucoprotein alpha subunit (*CGA*, Vglut2^{flox}: 100 ± 17.47 %; LepRb$^{\Delta Vglut2}$: 245.3 ± 89.91 %; t_8 = 1.20; p=0.26) relative to actin b (*Actb*) expression was similar between genotypes. Mediobasal hypothalamic expression of *Kiss1*, *Pdyn*, *Kiss1r*, and *Tac3r* relative to β-2-microglobulin (*B2m*) expression was similar between control and experimental females (Fig 6J-M). However, relative *Tac2* expression was about 50% lower in LepRb$^{\Delta Vglut2}$ compared to controls (Fig 6N).

The action of LepRb PMv neurons in sexual maturation requires glutamate

In previous studies, we showed that endogenous re-expression of LepRb in the PMv induced puberty and improved fertility of LepRb null mice (Donato et al., 2011; Mahany et al., 2018). To evaluate if glutamate neurotransmission is required for leptin-induced pubertal development, we produced a dual-floxed mouse model. Lepr^{loxTB} mice that lacks LepRb were crossed with a Vglut2^{flox} line, to generate the LepR^{loxTB};Vglut2^{flox} mice in which delivery of Cre restores *Lepr* while deleting *Vglut2*.

The Lepr^{loxTB} mice show no leptin-induced pSTAT3-ir (Fig 7A-B, Q, S). Expression of *Vglut2* mRNA is intact in these mice despite the lack of leptin signaling (Fig 7C-D). These mice are obese and infertile, have reduced uterine size, and no ovarian corpora lutea (Fig 7E-H, T). As observed previously (Mahany et al., 2018), Lepr^{loxTB} mice with reexpression of LepRb in the PMv (Lepr^{loxTB} AAV-Cre) show leptin-induced pSTAT3-ir in the PMv (Fig. 7I, Q). Expression of *Vglut2* mRNA is intact in these mice (Fig. 7J) and they have increased uterine size and ovarian corpora lutea (Fig. 7K, L, T) indicating successful ovulation. The LepR^{loxTB} was used as the negative control, the LepR^{loxTB} with injection of AAV-Cre into the PMv was used as positive control for the procedure and the wild-type littermate was used as the positive control for the undisturbed morphology of the hypothalamus and the reproductive organs.

We obtained six LepR^{loxTB};Vglut2^{flox} female mice with AAV-Cre centered in the PMv and two mice with AAV-Cre outside the PMv. Reexpression of LepRb was confirmed by the presence of leptin-induced pSTAT3-ir in the PMv neurons and the deletion of Vglut2 was confirmed by a decreased *Vglut2* (*Slc17a6*) mRNA expression, compared to the LepR^{loxTB} with AAV-Cre. Mice with successful injections (n=6) showed an increased number of leptin-induced pSTAT3-ir neurons, similar to that obtained in AAV-Cre injected LepR^{loxTB} (Fig7M, Q). Mice with AAV-Cre injections outside the PMv (n=2) showed pSTAT3-ir in adjacent nuclei, i.e., dorsomedial and ventromedial nuclei of the hypothalamus and were removed from the analysis. Variable contamination of the Arc was evident but the number of pSTAT3-ir was similarly negligible in AAV-Cre injected LepR^{loxTB} and LepR^{loxTB};Vglut2^{flox} mice (Fig 7I, M, S). Comparing AAV-Cre injected groups, *Vglut2* mRNA was decreased only in LepR^{loxTB};Vglut2^{flox} mice with injections successfully targeting PMv neurons (Fig 7N, R).

Correctly PMv injected LepR^{loxTB};Vglut2^{flox} mice showed no sign of puberty onset (vaginal opening) and no pregnancy until the end of the experiment (about 60 days). Histological examination showed these mice had reduced uterine size and no corpora lutea suggesting low estradiol, lack of sexual maturation and ovulation (Fig 7O, P, T)

These findings demonstrate that glutamate neurotransmission is required for leptin action in pubertal development and reproductive function mediated by PMv neurons.

DISCUSSION

Understanding the role of leptin in the control of reproduction has largely advanced in the last few years, but many open questions remain regarding the neural pathways and the molecular mechanisms involved. While overlapping neural pathways exist, the PMv has arisen as an essential hub in this circuitry. The PMv is a glutamatergic nucleus (Donato et al., 2011; Vong et al., 2011) rich in leptin responsive cells (Leshan et al., 2009; Louis et al., 2011; Scott et al., 2009; Williams et al., 2011). Nevertheless, recent studies have shown that deletion of LepRb in glutamatergic cells does not disrupt puberty or fertility, as opposed to large reproductive deficits when LepRb is deleted from GABAergic cells (Martin et al., 2014; Zuure et al., 2013). We have therefore investigated in more detail the role of glutamatergic neurotransmission in LepRb PMv neurons.

Leptin treatment prevents a fall in LH levels in states of negative energy balance in rodents and humans (Ahima et al., 1996; Chan et al., 2003; Donato et al., 2009; Welt et al., 2004). In ob/ob (*Lep*^{ob}) mice, which are infertile and hypogonadotropic, leptin administration increases LH levels, while this treatment is ineffective in PMv lesioned *Lep*^{ob} mice (Donato et al., 2011), indicating that intact PMv is required for the leptin stimulatory effect on LH in leptin-deficient mice. In the current study, we expanded this observation showing that in fed mice, acute unilateral activation of leptin responsive PMv neurons using stimulatory DREADDs transiently elevated LH levels in a normal nutritional state (ie. not in negative energy balance). This increase was correlated with the number of activated PMv LepRb neurons, and it was only observed following a substantial neuronal stimulation (cFos activation). The animals that did not show an LH increase despite having the virus targeted to the PMv had low cFos-ir in the PMv, possibly due to virus inactivity or low CNO entry into the brain (Gomez et al., 2017).

It is well accepted that clozapine has high affinity to DREADDs (Gomez et al., 2017). Thus, the hM3Dq injected animals showing clozapine-induced LH release strongly support our observations using CNO, i.e. targeted activation of PMv neurons leads to increase in circulating LH. Of note, optogenetic activation of a pituitary adenylate-cyclase-activating polypeptide (PACAP) expressing subpopulation of PMv neurons leads to increased activity of kisspeptin neurons. Whether this increases LH release is not known. Instead, the authors showed that deletion of PACAP in the PMv leads to an exacerbation of LH response to acute leptin

administration (Ross et al., 2018), what reinforces the role of LepRb PMv neurons in LH secretion. Further studies are required to define the interaction between glutamate and PACAP neurotransmission in downstream targets of PMv neurons.

The use of stereotaxic injections inevitably leads to heterogeneity in the injection sites. The main caveat to our study was the activation in some animals of neighboring hypothalamic areas containing leptin receptor, abundant in the mediobasal hypothalamus (Louis et al., 2011; Scott et al., 2009). Larger injections in a few animals, and perhaps the presence of dendrites from LepRb neurons adjacent to PMv, led to contamination of other sites, mainly the Arc. For this reason, we investigated the distribution of cFos-ir in Arc neuronal populations involved in stimulation of LH secretion (i.e., POMC and kisspeptin).

POMC neurons have been involved in modulation of the reproductive axis (Leranth et al., 1988; Manfredi-Lozano et al., 2016; Scimonelli and Celis, 1990). The POMC-derived peptide α-melanocyte-stimulating hormone (αMSH) has a stimulatory role on reproduction via actions on kisspeptin and GnRH neurons (Manfredi-Lozano et al., 2016; Roa and Herbison, 2012). Therefore, direct activation of POMC neurons, although small in number, may have contributed to the higher LH peak observed in these animals. On the other hand, kisspeptin is a direct stimulator of GnRH but only about 10% of KNDy neurons in the Arc express LepRb (Cravo et al., 2013, 2011; Donato et al., 2011; Louis et al., 2011; True et al., 2011). Restoration of LepRb in kisspeptin neurons does not restore fertility in *Lepr* deficient mice (Cravo et al., 2013, 2011). The very low number of cFos-ir KNDy neurons we observed makes it unlikely that contamination or downstream activation of KNDy neurons contributed to the LH secretion. Of note, in kisspeptin signaling deficient mice, glutamate receptor agonists induce LH secretion, indicating that alternative glutamatergic pathways bypass KNDy neurons to regulate the reproductive axis (Garcia-Galiano et al., 2012). Uncharacterized mCherry-expressing cFos neurons were observed in the posterior Arc, but lack of prior knowledge of a role in reproduction curtails the evaluation of a plausible role in LH release.

Due to lack of a specific model to target the PMv neurons, we investigated the reproductive phenotype in animals with Vglut2 deletion in LepRb expressing neurons, rendering them incapable of transmitting fast-acting downstream signals (Xu et al., 2013). These animals develop obesity (Xu et al., 2013). To avoid the effects of high adiposity in reproductive outcome,

body weight was monitored during all reproductive phenotype assessment. While the reproductive effect in males was not obvious, LepRb-cre$^{\Delta Vglut2}$ females showed delayed pubertal completion and blunted estrous cycles. The reproductive deficits were observed prior to the manifestation of any changes in body weight, indicating that these alterations are independent of metabolic dysregulation (Donato et al., 2011). It is important to stress that Vglut2 is expressed in several other LepRb neurons including the dorsomedial and the ventromedial nuclei of the hypothalamus (Xu et al., 2013). Based on extensive literature and circuit tracing, the PMv remains the prime candidate to relay leptin's effect in reproductive function.

To test if glutamatergic signaling in LepRb PMv neurons is required for sexual maturation we studied LepR-null;Vglut2-floxed females. This strategy aimed to "bypass" the potential redundancy played by alternative neural pathways. Our prior studies showed that selective re-expression of LepRb in the PMv induced puberty and fertility in LepR-null females (Donato et al., 2011; Mahany et al., 2018). Here we observed that deletion of Vglut2 in PMv neurons blocked this effect. Female gonads remained in a prepubertal state, with undeveloped uterine horns and no corpora lutea in the ovaries.

Despite prior reports showing that lack of leptin signaling in glutamatergic cells has no effects on reproduction (Martin et al., 2014; Zuure et al., 2013) we show that glutamatergic neurotransmission in leptin responsive cells of the PMv is necessary for typical pubertal development and reproduction. Due to the fundamental role of reproduction for species survival, redundancy of neural pathways is expected, and developmental adaptations may have occurred in those studies. Of note, a recent study showed that re-expression of LepRb only in GABAergic cells is not sufficient for restoration of reproduction in otherwise LepRb null mice, emphasizing the need for other populations (Quaresma et al., 2021). Similarly, alternative metabolic signals may take over control in the absence of leptin signaling in this specific pathway (Hill et al., 2010; Hill and Elias, 2018).

Leptin depolarizes about 75% of PMv LepRb neurons (Williams et al., 2011). Depolarizing glutamatergic neurons may directly activate downstream neurons. The LepRb PMv neurons project to the preoptic area, where they directly contact GnRH neurons (Leshan et al., 2009; Louis et al., 2011). Alternatively, LepRb neurons may activate astrocytes, which in turn stimulate GnRH neurons and LH pulsatility (Vanacker et al., 2021) or GnRH fibers at the

median eminence (Donato et al., 2011). In fact, LepRb-cre$^{\Delta Vglut2}$ females showed increased GnRH-ir fibers located in the adjacencies of the median eminence. In these females, LH release in response to kisspeptin was reduced suggesting peptide retention and deficits in GnRH release. Similar results were obtained after reactivation of leptin signaling in the PMv of LepRb-null mice (Donato et al., 2011). In *Lep*^{ob} mice, GnRH fiber density is higher, but it decreases following leptin injection (Bellefontaine et al., 2014). A large density of synaptic contacts exists in the GnRH terminals in the vicinity of the ME, and specific inhibition of these terminals blocks LH pulses (Wang et al., 2020). We did not observe alterations in gonadotropin expression in the pituitary gland, but we found a reduction in *Tac2* levels, coding for Neurokinin B, in the hypothalamus of LepRb-cre$^{\Delta Vglut2}$ females. These findings indicate that blockade of glutamatergic neurotransmission in LepRb neurons disrupts key components of the GnRH pulse generator (Han et al., 2023; Ruka et al., 2013; Uenoyama and Tsukamura, 2023), leading ultimately to reproductive deficits.

LepRb PMv neurons also project to the Arc and AVPV, where they contact Kiss1 neurons (Donato et al., 2011; Ross et al., 2018). However, the interaction and dynamics between the PMv and the kisspeptin populations remain unclear. In rats, the proestrus increase in *Kiss1* mRNA and cFos-ir in AVPV is blunted following bilateral lesions of the PMv. In the Arc, *Kiss1* mRNA is not altered during a leptin induced LH peak or in PMv lesioned animals (Donato et al., 2009, 2013). In mice, Arc Kiss1 neurons are downstream of PACAP PMv neurons in reproductive function (Ross et al., 2018). Thus, complementary to fast acting glutamatergic neurotransmission, neuropeptides released from PMv cells contribute to the long-term regulation of reproduction by leptin and its integration with other modulatory signals, e.g., the neuropeptide PACAP (Evans et al., 2023; Ross et al., 2018).

Further studies are required for better characterization of downstream pathways and mechanisms linking glutamatergic and neuropeptidergic neurotransmission from LepRb neurons in reproductive function.

MATERIALS and METHODS

Animals

The Lepr-null (*LepR*^{loxTB}, kindly provided by Dr. Elmquist, UTSW Medical Center, Dallas, TX, available in JAX®, stock 018989) (Berglund et al., 2012), the *Lepr*^{Cre} knock-in (LepRb-Cre, JAX®; stock 032457) (Leshan et al., 2006), Kiss1-hrGFP (JAX®, stock 023425) (Cravo et al., 2013), Vglut2^{flox} (*Vglut2* or *Slc17a6* gene, JAX®; Stock 012898) (Tong et al., 2007) and C57BL/6 (JAX®; Stock 000664) mice were used for experiments. They were held in a 12:12 light:dark cycle (lights on at 6AM), temperature-controlled (21-23°C) environment with *ad libitum* access to water and food. Mice were fed a low-phytoestrogen diet (Envigo 2016 diet) and a higher protein and fat phytoestrogen reduced diet (Envigo 2019 Teklad diet) when breeding. A phytoestrogen-reduced diet was used to avoid the exogenous effect of estrogen on reproductive physiology. Animals were bred and housed in our colony under the guidelines of the University of Michigan IACUC (PRO00010420). Procedures and experiments were carried out in accordance with the guidelines established by the National Institutes of Health "Guide for the Care and Use of Laboratory Animals" and approved by the University of Michigan Committee on Use and Care of Animals.

Stereotaxic injections

Unilateral stereotaxic injections of AAV-Cre/GFP (AAV-Cre) and AAV-GFP (Vector Core, University of North Carolina) in LepR^{loxTB}, LepR^{loxTB};Vglut2^{flox} and wild type females, and unilateral stereotaxic injections of pAAV8-hSyn-DIO-hM3D(Gq)-mCherry (AAV-hM3Dq, Addgene plasmid # 44361) (Krashes et al., 2011) from Bryan Roth, and of pAAV8-hSyp-DIO-mCherry (AAV-mCherry, Addgene plasmid # 50459) in LepRb-Cre females were performed using a picospritzer attached to a glass pipette under isoflurane anesthesia in a stereotaxic apparatus (Kopf), (Sáenz de Miera et al., 2023). The stereotaxic coordinates for injection in PMv, measured from the rostral rhinal vein were [anteroposterior: -0.54], the exposed superior sagittal sinus [mediolateral: ± 0.05], and from the top of the dura-mater [dorsoventral -0.54]. Mice were followed twice daily for the first 3 days after surgery and daily for 7 more days for appropriate recovery. Experiments were performed 1 month after surgery.

Activation of PMv LepRb neurons and its effect on LH release

Adult LepRb-Cre females (8-10 weeks old) received unilateral stereotaxic injections of ~50nl of AAV-hM3Dq in the PMv. One-month later mice were transferred to the Mouse Metabolic

Phenotyping Center-Live (U2C – NIDDK) where they were cannulated in the aortic artery for serial blood sampling and the jugular vein for intravenous (iv.) injections (Sáenz de Miera et al., 2023). They were then connected to the Culex Automated Blood Sampling System 3 days after surgery. The following day, 3 blood samples were taken every 10 min to establish baseline hormonal levels, followed by iv. injection of either CNO (n=19) or clozapine (n=4) at (0.5mg/kg in 50µl, time 0). All injections were performed at the same time of the day, 1:00PM. Blood samples were sequentially taken following the injection every 10 min for 1h. A negative control group received a stereotaxic injection of AAV-mCherry then a month later they were cannulated and the same protocol for blood collection was used. These animals received an injection of CNO on the day of the experiment (n=5). An additional group of LepRb-Cre females with no AAV injections were cannulated and received an iv. injection of clozapine (n=7) and were used as additional controls for blood collection. All animals were disconnected from the sampling system 2h after injection, a vaginal smear was collected to assess the phase of the estrous cycle and they were perfused under isoflurane anesthesia. Brains were collected and processed for histology. Blood samples were removed from the Culex machine immediately following the 2-hour mark and kept on ice. Samples were centrifuged at 14,000 g for 30 seconds at 4 °C and plasma removed and stored at -80 °C until hormone analysis.

Assessment of body weight and reproductive phenotype

To inactivate glutamate in leptin responsive cells, LepRb-Cre mice were crossed with mice carrying loxP-modified Vglut2 alleles. Our experimental mice were homozygous for the LepRb-Cre allele (LepRb$^{cre/cre}$) and homozygous for the Vglut2-loxP allele (Vglut2$^{fl/fl}$). Our controls consisted of mice homozygous for the Cre allele (LepRb$^{cre/cre}$;Vglut2$^{+/+}$, named LepRb-Cre) or homozygous for the Vglut2-loxP allele (LepRb$^{+/+}$;Vglut2$^{fl/fl}$, named Vglut2^{flox}). Both experimental (LepRb$^{cre/cre}$;Vglut2$^{fl/fl}$, named LepRb$^{\Delta Vglut2}$) and control mice were derived from the same litters with parents homozygous for one of the genes and heterozygous for the other gene (LepRb$^{cre/cre}$;Vglut2$^{fl/+}$ or LepRb$^{cre/+}$;Vglut2$^{fl/fl}$). Mice were genotyped at weaning (21 days) and again at the end of the experiments.

Timing of puberty onset was monitored daily in experimental (LepRb$^{\Delta Vglut2}$) and control (LepRb-Cre) mice for external signs of puberty (n=7-13). In females, vaginal opening was monitored from postnatal day 19 (P19), followed by the timing for the occurrence of first estrus, a sign of

puberty completion defined by the identification of keratinized cells for 2 consecutive days after 2 previous days with leukocytes in the vaginal lavage or by an estrus stage preceded by a proestrus stage (García-Galiano et al., 2017). In males, the day of balanopreputial separation was monitored from P25. Body weight for each animal was obtained on the day these events were observed. Animals were grown in normalized litters (5-7 pups/litter). Estrous cycles were assessed in young adult virgin mice. Females were housed with proven male breeders and monitored for fertility, latency to pregnancy, and number of pups per litter. Body weight of adult male and female mice was monitored weekly from 13 to 26 weeks of age. At the end of the experiment, total body weight, body fat and lean mass were measured in conscious mice using a nuclear magnetic resonance-based analyzer (EchoMRI, 4in1-900).

Kisspeptin injections

Adult LepRb-Cre and LepRb$^{\Delta Vglut2}$ females (3-6 mo) were transferred to the Mouse Metabolic Phenotyping Center-Live where they were cannulated in the aortic artery for serial blood sampling. Blood samples for baseline LH were taken every 7 minutes for 30 minutes before the injection. They then received an ip. injection of kisspeptin 65µg/kg (Kisspeptin-10, #048-56 Phoenix Pharmaceuticals) (Wang et al., 2019) and blood was then sampled every 7 minutes for 30 min.

Endogenous reexpression of *Lepr* and concomitant deletion of *Vglut2* in PMv neurons

The LepR null (LepR^{loxTB}) mouse model has a loxP-flanked transcription-blocking cassette (loxTB) inserted between exons 16 and 17 of the *Lepr* gene (Berglund et al., 2012; Donato et al., 2011). The LepR^{loxTB} mice lack the LepR intracellular domain and are obese, diabetic, and infertile. Cre-mediated excision of loxP sites generates LepR with signaling capacity. The LepR^{loxTB} mice were crossed with the Vglut2-floxed mice, which carry loxP sites flanking exon 2 of *Vglut2*, to generate the LepR^{loxTB};Vglut2^{flox} allowing for Cre-induced restoration of LepR and deletion of Vglut2 in PMv neurons. Mice were monitored for puberty and fertility as described above. Sixty days after introduction of the male breeders, females were anesthetized, perfused and brains were processed as described below.

Unilateral stereotaxic injections of AAV-Cre were used to restore LepR signaling in the PMv in homozygous LepR^{loxTB} 7 to 10-week-old females mice (previously described in Mahany et al.,

2018) to restore LepR signaling and to selectively delete *Vglut2* in the PMv of LepR^{loxTB};Vglut2^{flox} homozygous females (n=9). An additional cohort of LepR^{loxTB} was injected with AAV-Cre and included as positive control (n=5). WT mice were used as positive (fertile) controls (n=13, six with AAV-GFP injection; seven without injections) (Mahany et al., 2018) and LepR^{loxTB} (LepR-null, n=4) mice were used as negative (infertile) controls. Six to eight weeks after surgery, animals were ip. injected with leptin (3mg/kg) 1.5 h before perfusion. Brain, uterus, and ovaries were collected. Reproductive maturation was assessed by vaginal opening, uterus size and presence of ovarian corpus lutea. Brain tissue was processed for GFP immunohistochemistry and *Vglut2 in situ* hybridization (ISH).

Tissue Collection and Histology

Mice were deeply anesthetized with isoflurane (Fluriso, VetOne) and intracardially perfused with 0.1M phosphate buffered saline (PBS) followed by 10% normal buffered formalin. Brains were dissected and kept in post-fixative (20% sucrose in fixative) for 4 h and cryoprotected overnight in 20% sucrose in PBS. Brains were cut into 4 series of 30 µm coronal sections using a freezing microtome (Leica SM 2010R) and stored at -20°C in cryoprotectant until used. Brains of animals treated with leptin were postfixed for only 2 h and were processed for pSTAT3-ir to validate LepRb re-expression (Münzberg et al., 2003; Williams et al., 2011). Reproductive organs were fixed in 10% formalin and processed using paraffin-embedded protocol and H&E staining (Donato et al., 2011; Mahany et al., 2018).

Immunofluorescence

Floating sections were rinsed with PBS and blocked with 3% normal donkey serum in PBS + 0.25% Triton-X 100 for 1 hour at room temperature. Sections were incubated overnight at 4°C with primary antibodies in blocking buffer. Primary antibodies used are listed in Table 2. Sections were rinsed and incubated with secondary antibodies for 1 hour and rinsed in PBS. Secondary antibodies used are listed in Table 2. Sections were mounted on gelatin-precoated slides and coverslipped with Fluoromont-G (Electron Microscopy Sciences) mounting medium.

pSTAT3 immunoreactivity was performed to assess reactivation of functional leptin receptor. Brain sections were pretreated with 30% H_2O_2 to block endogenous peroxidase activity, 0.3% glycine and 0.03% sodium dodecyl sulphate (SDS) prior to primary antibody incubation. Tissue

was blocked in 3% normal donkey serum + 0.25% Triton in PBS for 1 hour and incubated in primary rabbit anti-pSTAT3 (Table 2) for 48 hours at 4°C. Primary antibody was detected using a biotinylated secondary antibody (Table 2) by avidin-biotin peroxidase method (ABC Kit, Vector Laboratories) using diaminobenzidine (DAB; Sigma) as chromogen.

In situ **hybridization (ISH)**

Single ISH was performed to determine deletion of *Vglut2* in PMv neurons (n=9 experimental vs n=4 control). Briefly, a series of brain sections were mounted onto SuperFrost plus slides (ThermoFisher Scientific), fixed in 10% NBF for 20 minutes and cleared with xylene for 15 minutes. Slides were boiled in sodium citrate buffer (pH 6.0) for 10 min. The *Slc17a6* DNA template was generated from mouse hypothalamic RNA by PCR amplification. The following primers were used to amplify a 909 base-pair sequence in the gene encoding *Vglut2* (exon 2 of the *Scl7a6* gene): Forward (5' CCGGGGAAAGAGGGGATAAAG 3') and reverse (5' GTAGACGGGCATGGATGTGA 3'). The antisense radio-labeled ^{35}S-*Vglut2* riboprobe was generated by *in vitro* transcription using a T7 RNA polymerase (Promega). ^{35}S-labeled riboprobe was diluted in hybridization solution (50% formamide, 10 mM Tris-HCl pH 8.0, 5 mg tRNA, 10 mM dithiothreitol/DTT, 10% dextran sulfate, 0.3 M NaCl, 1 mM EDTA, and 1× Denhardt's solution), and brain slices were hybridized overnight at 57 °C. Slides were then incubated in 0.002% RNase A followed by stringency washes in SSC (sodium chloride-sodium citrate buffer). Sections were dipped in NTB autoradiographic emulsion (Kodak) and stored in light-protected slide boxes at 4°C for 2 weeks. Signal was developed with developer and fixer (Carestream, Rochester, NY, USA), and the slides were cover-slipped with DPX (Electron Microscopy Sciences) mounting medium.

To confirm the deletion of *Vglut2* in *LepRb* neurons we did chromogenic ISH using BaseScope Duplex^{TM} (n=4 LepRb-Cre vs n=4 LepRb$^{\Delta Vglut2}$). Fresh frozen 16µm coronal sections were collected on Superfrost Excell slides (Fisher) and stored at -80°C. Tissue sections were fixed in 10% NBF for 30 min and then dehydrated with a series of graded alcohols. The rest of the procedure was done with BaseScope Duplex Reagent Kit (ACD, #323800). Briefly, endogenous peroxidase was blocked with H_2O_2 for 10 minutes and tissue was digested with Protease IV for 10 min at room temperature. Sections were hybridized with BaseScope probes targeting LepR (BA-Mm-Lepr-1zz-st, catalog # 895341) and a probe designed against exon 2 of *Vglut2* (BA-

Mm-Slc17a6-1zz-st-C2, # 1240891-C2) for 2h at 40°C. Following hybridization, amplification and detection were done using the BaseScope Duplex Detection Reagents ACD, #323810, and probes were detected using Green (*LepR*) and Fast Red (*Vglut2*) and counterstained with 50% Gill's Hematoxylin for 30 s.

Quantitative PCR (qPCR)

Vglut2^{flox} (n=7) and LepRb$^{\Delta Vglut2}$ (n=5) females in diestrus were euthanized to collect blood for basal LH analysis and dissect tissues for qPCR. Fresh frozen pituitaries and mediobasal hypothalamus were homogenized in Qiazol (Qiagen) and total RNA was extracted using chloroform and precipitated with isopropanol. Complementary DNA (cDNA) was synthetized using MultiScribe™ reverse transcriptase and random primers (Invitrogen) from 1.5 or 2 µg of RNA and diluted to 10ng/µl. Gene expression was analyzed by qPCR in 20ng of cDNA in triplicate 10 µl reactions using SYBR Green Taq MasterMix (Bio-Rad), following the manufacturer's instructions in a CFX-384 Real-Time PCR thermocycler (Bio-Rad). The primers used are specified in Table 3. mRNA expression in mutant vs control samples was determined using relative gene copy numbers by the comparative threshold (Ct) method. The fold gene expression was calculated as $2^{-\Delta\Delta Ct}$ and shown as a percentage of relative gene expression in the control group.

Hormone profile

For LH assay, sera were sent to the University of Virginia Ligand Assay and Core of the Center for Research in Reproduction (Charlottesville, Virginia, USA), where serum LH was measured by ultra-sensitive LH ELISA. This in-house method is based on Steyn (Steyn et al., 2013). The capture monoclonal antibody (anti-bovine LH β subunit, 518B7) was provided by Janet Roser, University of California. The detection polyclonal antibody (rabbit LH antiserum, AFP240580Rb) was provided by the National Hormone and Peptide Program (NHPP). HRP-conjugated polyclonal antibody (goat anti-rabbit) was purchased from DakoCytomation (Glostrup, Denmark; D048701-2). Mouse LH reference prep (AFP5306A; NHPP) was used as the assay standard. The Limit of Quantitation (Functional Sensitivity) was defined as the lowest concentration that demonstrates accuracy within 20% of expected values and intra-assay coefficient of variation (%CV) <20% and was determined by serial dilutions of a defined sample

pool. Intra-assay %CV is 2.2%. Inter-assay %CVs were 7.3% (Low QC, 0.13 ng/ml), 5.0% (Medium QC, 0.8 ng/ml) and 6.5% (High QC, 2.3 ng/ml). Functional sensitivity was 0.016 ng/ml. with an assay reportable range of 0.016 - 4.0 ng/ml and intra-assay CV of 6.24%.

Image and data analysis

Photomicrographs were acquired using Axio Imager M2 (Carl Zeiss Microscopy). Confocal microscopy images were acquired using NIS-Elements on a Nikon N-SIM + A1R microscope with a resonance scanner. For cell quantification 40× images were used. Neuronal counting and coexpression analysis were done using the "Freehand selection" tool to outline the areas of interest and the "Multi-point selection" and "Region of Interest manager" tools in ImageJ (NIH) to compare the same neurons across different color channels. Sections containing the PMv were analyzed (Bregma ~ -2.3/-2.70, Paxinos Brain atlas) and adjacent nuclei were also analyzed to determine the degree of viral contamination. Quantification of GnRH fibers was performed in 2 consecutive 20X images of the Arcuate nucleus (Bregma ~ -2.06, Paxinos Brain atlas). For each image a background value was measured and subtracted from the image. A 250µm wide x 140µm high rectangle was placed on the edge of the 3V wall to cover Arc GnRH-ir, carefully avoiding the saturated expression in the tuberoinfundibular sulcus region, and integrated density (mean pixel intensity x area) of the signal was quantified.

Data are expressed as mean ± SEM. Data were assessed for normality. When data did not fit a normal distribution, they were transformed and analyzed by a parametric test or analyzed using a non-parametric test. Unpaired 2-tailed Student's t test was used for comparison between 2 groups. For AUC of LH levels after CNO/clozapine, baseline LH level was brought to 0, subtracting the -10 min LH value from all the timepoints for each animal. Then, AUC analysis was performed and only the positive area was considered for analysis. One-sample t-test analysis was used comparing data to a theoretical mean of 0. LH levels after kisspeptin injection were analyzed using AUC. One-way ANOVA was used to compare 3 or more groups. Body weight data was analyzed using repeated-measures 2-way ANOVA followed by Sidak's post-hoc multiple comparison test. A P value less than 0.05 was considered significant. Excel software (Microsoft, Inc.) was used to organize and calculate data. Statistical analyses and graphs were performed using GraphPad Prism v.7 (GraphPad software, Inc.). Photoshop CS6 (Adobe, Inc.)

was used to integrate graphs and digital images into figures. Only brightness, contrast, and levels were modified to improve data visualization.

DECLARATION

The authors declare that no competing financial interests exist.

ACKNOWLEDGEMENTS

The Michigan Mouse Metabolic Phenotyping Center-Live is supported by NIH Center Grant U2C DK135066 (Mi-MMPC), P30 DK020572 (MDRC) and P30 DK089503 (MNORC), and the Ligand Assay and Analysis Core – University of Virginia is supported by R24 grant HD102061. This work was supported by R01 HD069702 and R21 HD109485 grant to CFE, NIH R01DK056731 to MGM, and URM Pilot Grant from P30 DK089503 (MNORC) to CSM.

BIBLIOGRAPHY

Ahima RS, Prabakaran D, Mantzoros C, Qu D, Lowell B, Maratos-flier E, Flier JS. 1996. Role of leptin in neuroendocrine response to fasting. *Nature* **382**:250–2.

Bellefontaine N, Chachlaki K, Parkash J, Vanacker C, Colledge W, d'Anglemont de Tassigny X, Garthwaite J, Bouret SG, Prevot V. 2014. Leptin-dependent neuronal NO signaling in the preoptic hypothalamus facilitates reproduction. *J Clin Invest* **124**:3678–3678. doi:10.1172/jci77652

Berglund ED, Vianna CR, Jr JD, Kim MH, Chuang J, Lee CE, Lauzon DA, Lin P, Brule LJ, Scott MM, Coppari R, Elmquist JK. 2012. Direct leptin action on POMC neurons regulates glucose homeostasis and hepatic insulin sensitivity in mice. *J Clin Invest* **122**:1000–1009. doi:10.1172/JCI59816DS1

Biro FM, Khoury P, Morrison JA. 2006. Influence of obesity on timing of puberty. *Int J Androl* **29**:272–7. doi:10.1111/j.1365-2605.2005.00602.x

Boehm U, Zou Z, Buck LB. 2005. Feedback loops link odor and pheromone signaling with reproduction. *Cell* **123**:683–695. doi:10.1016/j.cell.2005.09.027

Bray GA, York DA. 1979. Hypothalamic and genetic obesity in Experimental Animals: An autonomic and endocrine hypothesis. *Physiol Rev* **59**:719–809.

Bronson F, Marsteller F. 1985. Effect of Short-term Food Deprivation on Reproduction in Female Mice. *Biol Reprod* **33**:660–7.

Burt Solorzano CM, McCartney CR. 2010. Obesity and the pubertal transition in girls and boys. *Reproduction* **140**:399–410. doi:10.1530/REP-10-0119

Cagampang F, Maeda K, Yokoyama A, Ota K. 1990. Effect of food deprivation on the pulsatile LH release in the cycling and ovariectomized female rat. *Horm Metab Res*. doi:10.1055/s-2007-1004900

Cameron JL, Weltzin TE, McConaha C, Helmreich DL, Kaye WH. 1991. Slowing of pulsatile luteinizing hormone secretion in men after forty-eight hours of fasting. *J Clin Endocrinol Metab* **73**:35–41.

Canteras NS, Simerly RB, Swanson LW. 1992. Projections of the ventral premammillary nucleus. *J Comp Neurol* **324**:195–212. doi:10.1002/cne.903240205

Chan JL, Heist K, DePaoli AM, Veldhuis JD, Mantzoros CS. 2003. The role of falling leptin levels in the neuroendocrine and metabolic adaptation to short-term starvation in healthy men. *J Clin Invest* **111**:1409–21. doi:10.1172/JCI200317490

Cravo RM, Frazao R, Perello M, Osborne-Lawrence S, Williams KW, Zigman JM, Vianna C, Elias CF. 2013. Leptin Signaling in Kiss1 Neurons Arises after Pubertal Development. *PLoS One* **8**. doi:10.1371/journal.pone.0058698

Cravo RM, Margatho LO, Osborne-Lawrence S, Donato J, Atkin S, Bookout AL, Rovinsky S, Frazão R, Lee CE, Gautron L, Zigman JM, Elias CF. 2011. Characterization of Kiss1 neurons using transgenic mouse models. *Neuroscience* **173**:37–56. doi:10.1016/j.neuroscience.2010.11.022

Czieselsky K, Prescott M, Porteous R, Campos P, Clarkson J, Steyn FJ, Campbell RE, Herbison AE. 2016. Pulse and surge profiles of luteinizing hormone secretion in the mouse. *Endocrinology* **157**:4794–4802. doi:10.1210/en.2016-1351

De Luca C, Kowalski TJ, Zhang Y, Elmquist JK, Lee C, Kilimann MW, Ludwig T, Liu SM, Chua SC. 2005. Complete rescue of obesity, diabetes, and infertility in db/db mice by neuron-specific LEPR-B transgenes. *J Clin Invest* **115**:3484–3493. doi:10.1172/JCI24059

Donato J, Cravo RM, Frazão R, Gautron L, Scott MM, Lachey J, Castro IA, Margatho LO, Lee S, Lee C, Richardson JA, Friedman J, Chua S, Coppari R, Zigman JM, Elmquist JK, Elias CF. 2011. Leptin's effect on puberty in mice is relayed by the ventral premammillary nucleus and does not require signaling in Kiss1 neurons. *J Clin Invest* **121**:355–368. doi:10.1172/JCI45106

Donato J, Silva RJ, Sita L V, Lee S, Lee C, Lacchini S, Bittencourt JC, Franci CR, Canteras NS, Elias CF. 2009. The ventral premammillary nucleus links fasting-induced changes in leptin levels and coordinated luteinizing hormone secretion. *J Neurosci* **29**:5240–50.

Donato JJ, Lee C, Ratra D, Franci C, Canteras N, Elias C. 2013. Lesions of the ventral premammillary nucleus disrupt the dynamic changes in kiss1 and gnrh expression

characteristic of the proestrus – estrus transition. *Neuroscience* **241**:67–79. doi:10.1016/j.neuroscience.2013.03.013

Evans MC, Wallace EG, Ancel CM, Anderson GM. 2023. Leptin, but not estradiol, signaling in PACAP neurons modulates puberty onset. *Endocrinology* **164**:bqad097.

Farooqi IS, Matarese G, Lord GM, Keogh JM, Lawrence E, Agwu C, Sanna V, Jebb SA, Perna F, Fontana S, Lechler RI, DePaoli AM, O'Rahilly S. 2002. Beneficial effects of leptin on obesity, T cell hyporesponsiveness, and neuroendocrine/metabolic dysfunction of human congenital leptin deficiency. *J Clin Invest* **110**:1093–103.

Farooqi IS, Wangensteen T, Collins S, Kimber W, Matarese G, Keogh JM, Lank E, Bottomley B, Lopez-Fernandez J, Ferraz-Amaro I, Dattani MT, Ercan O, Myhre AG, Retterstol L, Stanhope R, Edge JA, Mckenzie S, Lessan N, Ghodsi M, De Rosa V, Perna F, Fontana S, Barroso I, Undlien DE, O'Rahilly S. 2007. Clinical and Molecular Genetic Spectrum of Congenital Deficiency of the Leptin Receptor. *N Engl J Med* **356**:237–47.

García-Galiano D, Borges BC, Donato JJ, Allen SJ, Bellefontaine N, Wang M, Zhao JJ, Kozloff KM, Hill JW, Elias CF. 2017. PI3Kα inactivation in leptin receptor cells increases leptin sensitivity but disrupts growth and reproduction. *JCI Insight* **2**:e96728.

Garcia-Galiano D, Pineda R, Roa J, Ruiz-Pino F, Sanchez-Garrido MA, Castellano JM, Aguilar E, Navarro VM, Pinilla L, Tena-Sempere M. 2012. Differential modulation of gonadotropin responses to kisspeptin by aminoacidergic, peptidergic, and nitric oxide neurotransmission. *AJP Endocrinol Metab* **303**:E1252-63. doi:10.1152/ajpendo.00250.2012

Gomez JL, Bonaventura J, Lesniak W, Mathews WB, Sysa-Shah P, Rodriguez LA, Ellis RJ, Richie CT, Harvey BK, Dannals RF, Pomper MG, Bonci A, Michaelides M. 2017. Chemogenetics revealed: DREADD occupancy and activation via converted clozapine. *Science* **357**:503–507. doi:10.1126/science.aan2475

Han SY, Morris PG, Kim JC, Guru S, Pardo-Navarro M, Yeo SH, McQuillan HJ, Herbison AE. 2023. Mechanism of kisspeptin neuron synchronization for pulsatile hormone secretion in male mice. *Cell Rep* **42**:111914. doi:10.1016/j.celrep.2022.111914

Han X, Burger LL, Garcia-Galiano D, Sim S, Allen SJ, Olson DP, Myers MG, Elias CF. 2020.

Hypothalamic and Cell-Specific Transcriptomes Unravel a Dynamic Neuropil Remodeling in Leptin-Induced and Typical Pubertal Transition in Female Mice. *iScience* **23**:101563. doi:10.1016/j.isci.2020.101563

Hill JW, Elias CF. 2018. Neuroanatomical Framework of the Metabolic Control of Reproduction. *Physiol Rev* **98**:2349–80. doi:10.1152/physrev.00033.2017

Hill JW, Elias CF, Fukuda M, Williams KW, Berglund ED, Holland WL, Cho YR, Chuang JC, Xu Y, Choi M, Lauzon D, Lee CE, Coppari R, Richardson JA, Zigman JM, Chua S, Scherer PE, Lowell BB, Brüning JC, Elmquist JK. 2010. Direct Insulin and Leptin Action on Pro-opiomelanocortin Neurons Is Required for Normal Glucose Homeostasis and Fertility. *Cell Metab* **11**:286–297. doi:10.1016/j.cmet.2010.03.002

Krashes MJ, Roth BL, Lowell BB, Koda S, Ye C, Rogan SC, Adams AC, Cusher DS, Maratos-flier E. 2011. Rapid, reversible activation of AgRP neurons drives feeding behavior in mice. *J Clin Invest* **121**:1424–1428. doi:10.1172/JCI46229.1424

Leranth C, MacLusky N, Shanabrough M, Naftolin F. 1988. Immunohistochemical evidence for synaptic connections between pro-opiomelanocortin-immunoreactive axons and LH-RH neurons in the preoptic area of the rat. *Brain Res* **449**:167–76.

Leshan RL, Björnholm M, Münzberg H, Myers MGJ. 2006. Leptin Receptor Signaling and Action in the Central Nervous System. *Obesity* **14**:208S-212S.

Leshan RL, Louis GW, Jo YH, Rhodes CJ, Münzberg H, Myers MG. 2009. Direct innervation of GnRH neurons by metabolic- and sexual odorant-sensing leptin receptor neurons in the hypothalamic ventral premammillary nucleus. *J Neurosci* **29**:3138–3147. doi:10.1523/JNEUROSCI.0155-09.2009

Louis GW, Greenwald-Yarnell M, Phillips R, Coolen LM, Lehman MN, Myers MG. 2011. Molecular mapping of the neural pathways linking leptin to the neuroendocrine reproductive axis. *Endocrinology* **152**:2302–10.

Mahany EB, Han X, Borges BC, Da Silveira Cruz-Machado S, Allen SJ, Garcia-Galiano D, Hoenerhoff MJ, Bellefontaine NH, Elias CF. 2018. Obesity and High-Fat Diet Induce Distinct Changes in Placental Gene Expression and Pregnancy Outcome. *Endocrinology*

159:1718–1733. doi:10.1210/en.2017-03053

Manfredi-Lozano M, Roa J, Ruiz-Pino F, Piet R, Garcia-Galiano D, Pineda R, Zamora A, Leon S, Sanchez-Garrido MA, Romero-Ruiz A, Dieguez C, Vazquez MJ, Herbison AE, Pinilla L, Tena-Sempere M. 2016. Defining a novel leptin–melanocortin–kisspeptin pathway involved in the metabolic control of puberty. *Mol Metab* **5**:844–857. doi:10.1016/j.molmet.2016.08.003

Martin C, Navarro VM, Simavli S, Vong L, Carroll RS, Lowell BB, Kaiser UB. 2014. Leptin-Responsive GABAergic Neurons Regulate Fertility through Pathways That Result in Reduced Kisspeptinergic Tone. *J Neurosci* **34**:6047–6056. doi:10.1523/jneurosci.3003-13.2014

Moore AM, Abbott G, Mair J, Prescott M, Campbell RE. 2018. Mapping GABA and glutamate inputs to gonadotrophin-releasing hormone neurones in male and female mice. *J Neuroendocrinol* **30**:1–13. doi:10.1111/jne.12657

Münzberg H, Huo L, Nillni EA, Hollenberg AN, Bjørbæk C. 2003. Role of signal transducer and activator of transcription 3 in regulation of hypothalamic Proopiomelanocortin gene expression by leptin. *Endocrinology* **144**:2121–2131. doi:10.1210/en.2002-221037

Parfitt DB, Church KR, Cameron JL. 1991. Restoration of pulsatile luteinizing hormone secretion after fasting in rhesus monkeys (Macaca mulatta): Dependence on size of the refeed meal. *Endocrinology* **129**:749–756. doi:10.1210/endo-129-2-749

Porter DT, Goodman RL, Hileman SM, Lehman MN. 2021. Evidence that synaptic plasticity of glutamatergic inputs onto KNDy neurones during the ovine follicular phase is dependent on increasing levels of oestradiol. *J Neuroendocrinol* **33**:e12945. doi:10.1111/jne.12945

Quaresma PGF, Wasinski F, Mansano NS, Furigo IC, Teixeira PDS, Gusmao DO, Frazao R, Donato J. 2021. Leptin Receptor Expression in GABAergic Cells is Not Sufficient to Normalize Metabolism and Reproduction in Mice. *Endocrinology* **162**:1–16. doi:10.1210/endocr/bqab168

Quennell JH, Mulligan AC, Tups A, Liu X, Phipps SJ, Kemp CJ, Herbison AE, Grattan DR, Anderson GM. 2009. Leptin indirectly regulates gonadotropin-releasing hormone neuronal

function. *Endocrinology* **150**:2805–2812. doi:10.1210/en.2008-1693

Roa J, Herbison AE. 2012. Direct Regulation of GnRH Neuron Excitability by Arcuate Nucleus POMC and NPY Neuron Neuropeptides in Female Mice **153**:5587–5599. doi:10.1210/en.2012-1470

Ross RA, Leon S, Madara JC, Schafer D, Fergani C, Maguire CA, Verstegen AMJ, Brengle E, Kong D, Herbison AE, Kaiser UB, Lowell BB, Navarro VM. 2018. PACAP neurons in the ventral premammillary nucleus regulate reproductive function in the female mouse. *Elife* **7**:e35960. doi:10.7554/eLife.35960

Ruka KA, Burger LL, Moenter SM. 2013. Regulation of arcuate neurons coexpressing kisspeptin, neurokinin b, and dynorphin by modulators of neurokinin 3 and k-opioid receptors in adult male mice. *Endocrinology* **154**:2761–2771. doi:10.1210/en.2013-1268

Sáenz de Miera C, Feng J, Elias CF, Qi N. 2023. Remote Neuronal Activation Coupled with Automated Blood Sampling to Induce and Measure Circulating Luteinizing Hormone in Mice. *J Vis Exp* **198**:e65875. doi:10.3791/65875

Scimonelli T, Celis M. 1990. A central action of alpha-melanocyte-stimulating hormone on serum levels of LH and prolactin in rats. *J Endocrinol* **124**:127–32.

Scott MM, Lachey JL, Sternson SM, Lee CE, Elias CF, Friedman JM, Elmquist JK. 2009. Leptin targets in the mouse brain. *J Comp Neurol* **514**:518–532. doi:10.1002/cne.22025

Shamas S, Khan S, Yousaf M, Shabbir N, Zubair H, Shafqat S, Wahab F, Shahab M. 2015. Neuropeptides Fasting induced kisspeptin signaling suppression is regulated by glutamate mediated cues in adult male rhesus macaque (Macaca mulatta). *Neuropeptides* **52**:39–45. doi:10.1016/j.npep.2015.06.005

Steyn FJ, Wan Y, Clarkson J, Veldhuis JD, Herbison AE, Chen C. 2013. Development of a Methodology for and Assessment of Pulsatile Luteinizing Hormone Secretion in Juvenile and Adult Male Mice. *Endocrinology* **154**:4939–4945. doi:10.1210/en.2013-1502

Tong Q, Ye C, McCrimmon RJ, Dhillon H, Choi B, Kramer MD, Yu J, Yang Z, Christiansen LM, Lee CE, Soo Choi C, Zigman JM, Shulman GI, Sherwin RS, Elmquist JK, Lowell BB. 2007. Synaptic Glutamate Release by Ventromedial Hypothalamic Neurons Is Part of the

Neurocircuitry that Prevents Hypoglycemia. *Cell Metab* **5**:383–93. doi:10.1016/j.cmet.2007.04.001

True C, Kirigiti MA, Kievit P, Grove KL, Smith MS. 2011. Leptin is not the Critical Signal for Kisspeptin or Luteinising Hormone Restoration During Exit from Negative Energy Balance. *J Neuroendocrinol* **23**:1099–112. doi:10.1111/j.1365-2826.2011.02144.x

Uenoyama Y, Tsukamura H. 2023. KNDy neurones and GnRH/LH pulse generation: Current understanding and future aspects. *J Neuroendocrinol* e13285. doi:10.1111/jne.13285

Vanacker C, Defazio RA, Sykes CM, Moenter SM. 2021. A role for glial fibrillary acidic protein (Gfap)-expressing cells in the regulation of gonadotropin-releasing hormone (gnrh) but not arcuate kisspeptin neuron output in male mice. *Elife* **10**:e68205. doi:10.7554/eLife.68205

Vong L, Ye C, Yang Z, Choi B, Chua Jr SC, Lowell BB. 2011. Leptin Action on GABAergic Neurons Prevents Obesity and Reduces Inhibitory Tone to POMC Neurons. *Neuron* **71**:142–54.

Wang L, Guo W, Shen X, Yeo S, Long H, Wang Z, Lyu Q, Herbison AE, Kuang Y. 2020. Different dendritic domains of the GnRH neuron underlie the pulse and surge modes of GnRH secretion in female mice. *Elife* **9**:e53945. doi:10.7554/eLife.53945

Wang L, Vanacker C, Burger LL, Barnes T, Shah YM, Myers MG, Moenter SM. 2019. Genetic dissection of the different roles of hypothalamic kisspeptin neurons in regulating female reproduction. *Elife* **8**:e43999. doi:10.7554/eLife.43999

Welt CK, Chan JL, Bullen J, Murphy R, Smith P, DePaoli AM, Karalis A, Mantzoros CS. 2004. Recombinant human leptin in women with hypothalamic amenorrhea. *N Engl J Med* **351**:987–97.

Williams KW, Sohn J-W, Donato J, Lee CE, Zhao JJ, Elmquist JK, Elias CF. 2011. The acute effects of leptin require PI3K signaling in the hypothalamic ventral premammillary nucleus. *J Neurosci* **31**:13147–56. doi:10.1523/JNEUROSCI.2602-11.2011

Xu Y, Ran Kim E, Zhao R, Myers MGJ, Munzberg H, Tong Q. 2013. Glutamate release mediates leptin action on energy expenditure. *Mol Metab* **2**:109–115.

Yeo SH, Herde MK, Herbison AE. 2021. Morphological assessment of GABA and glutamate inputs to GnRH neurons in intact female mice using expansion microscopy. *J Neuroendocrinol* **33**:1–14. doi:10.1111/jne.13021

Zuure WA, Roberts AL, Quennell JH, Anderson GM. 2013. Leptin Signaling in GABA Neurons, But Not Glutamate Neurons, Is Required for Reproductive Function. *J Neurosci* **33**:17874–83. doi:10.1523/JNEUROSCI.2278-13.2013

FIGURES and TABLES

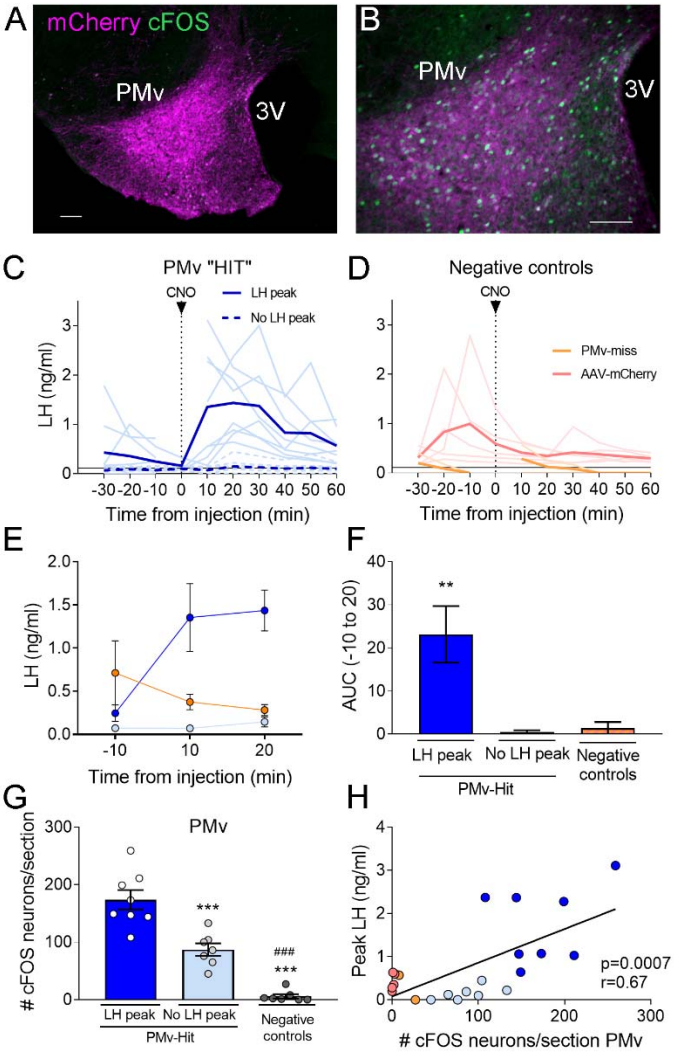

Figure 1. Chemogenetic activation of leptin receptor neurons in the ventral premammilary nucleus (PMv) induces luteinizing hormone (LH) release. A-B. Representative fluorescent photomicrographs of unilateral AAV-hM3Dq PMv injection. Low (A) and high (B) magnification of an animal correctly targeted to the PMv. Magenta: mCherry-immunoreactivity (-ir); Green: cFos-ir. **C.** LH levels in "PMv-hit" animals unilaterally expressing hM3Dq in the PMv following an intravenous (iv.) injection of clozapine-N-oxide (CNO) at time=0 (n=15). Continuous lines: animals showing an increase in LH had maximum LH levels ranging from 0.65-3.11 ng/ml. Dashed lines: animals showing no detectable increase in LH. Light blue lines represent individual values. Dark blue lines represent averaged values. **D.** LH levels in Negative

control animals (n=7), including “PMv-miss” (orange) and AAV-mCherry (pink) animals following an iv. injection of CNO at time=0. Light colored lines represent individual values. Dark colored lines represent average values. A gap is shown in the LH profile lines in animals that had a missing value at time 0 in C and D. **E.** Average LH levels at -10, 10 and 20 min for all 3 groups: “PMv-hit” with LH increase (n=8, dark blue), “PMv-hit” with no LH increase (n=7, light blue), Negative controls (including “PMv-miss” and AAV-mCherry, n=7, Orange). **F.** Positive area under the curve (AUC) of the values represented in E. One-sample t-tests (“PMv-hit” with LH increase: t_7=3.54, p = 0.009; “PMv-hit” with no LH increase: t_6=1.37, p = 0.22; Negative controls: t_6=1.00, p = 0.36), **p<0.01 compared to “0”. **G.** Number of cFos-ir neurons per section in the PMv in “PMv-hit” animals with (n=9) or without (n=7) an increase in LH and in Negative control animals, including “PMv-miss” and AAV-mCherry animals (n=7) 2h after the CNO injection (one-way ANOVA, $F_{2,19}$ = 81.66; p < 0.0001) **p<0.01 and ***p<0.001 vs. PMv-hit LH increase group; ###p<0.001 vs. PMv-hit no LH increase group. **H.** Correlation between the number of cFos-ir neurons per section in the PMv and the peak LH level in the 3 groups (Pearson r = 0.67; p = 0.0007). 3V: Third ventricle. Scale bars: 100µm.

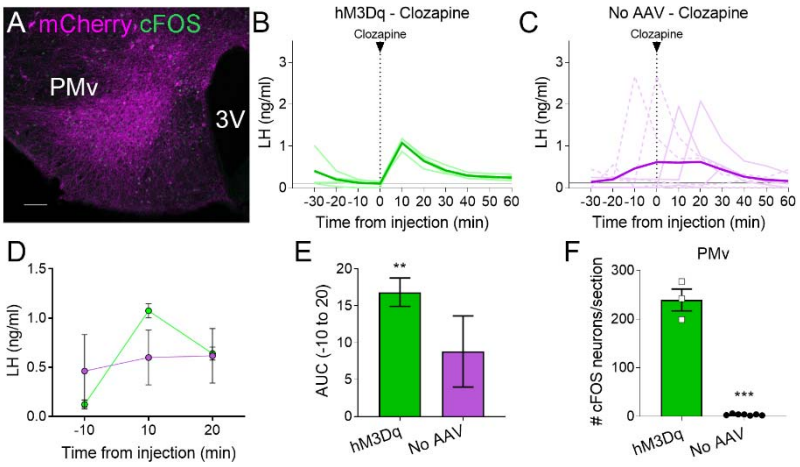

Figure 2. Clozapine induces cFos expression in the ventral premammillary nucleus (PMv) of animals expressing hM3Dq and luteinizing hormone (LH) release. A. Representative fluorescent photomicrograph of a unilateral AAV-hM3Dq PMv injection in a clozapine injected animal. Magenta: mCherry-immunoreactivity (-ir); Green: cFos-ir. **B.** LH levels in animals unilaterally expressing hM3Dq in the PMv following an iv. injection of clozapine at time=0 (n=4). Light green lines represent individual values. Dark green line represents averaged values. **C.** LH levels in animals not carrying any AAV following an iv. injection of clozapine at time=0 (n=7). Light magenta lines represent individual values. Dark magenta line represents averaged values. Continuous lines: animals with LH increase after the injection. Discontinuous lines: animals with no increase in LH after the injection. **D.** Average LH levels at -10, 10 and 20 min for both groups injected with clozapine. hM3Dq: green; No AAV: magenta. **E.** Positive area under the curve (AUC) of the values represented in D. One-sample t-tests (hM3Dq: t_3=8.79, p = 0.003; No AAV: t_6=1.83, p = 0.12), **p<0.01 compared to "0". **F.** Number of cFos-ir neurons per section of the PMv in AAV-hM3Dq and no AAV animals 2h after a clozapine injection (t_8 = 17.46; p < 0.0001). ***p<0.001 3V: Third ventricle. Scale bars: 100µm.

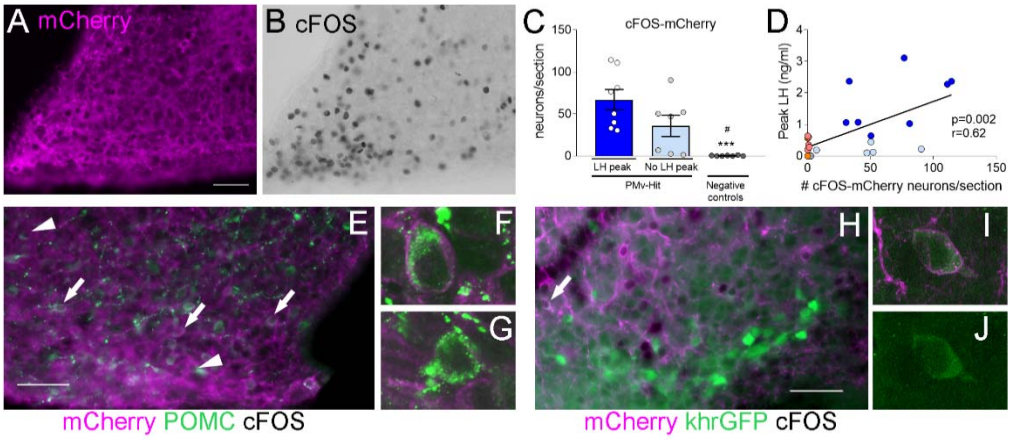

Figure 3. CNO-induction of luteinizing hormone (LH) secretion may have a mild contribution of POMC, but not KNDy, neurons. Representative images of **A.** mCherry-immunoreactivity (-ir) and **B.** cFos-ir of an animal with strong AAV contamination of the posterior Arc. **C.** Number of cFos-ir neurons with mCherry-ir colocalization per section in the posterior Arc in the 3 groups 2h after the CNO injection. (Kruskal-Wallis test = 14.63; $p < 0.0001$), ***$p<0.001$ vs. PMv-hit LH increase group, $^{\#}p<0.05$ vs. PMv-hit no LH increase group. **D.** Correlation between the number of mCherry-/cFos-ir neurons observed in the posterior Arc and the peak LH level in the 3 groups (Pearson $r = 0.62$; $p = 0.002$). **E.** POMC-ir (green) in a mouse with viral contamination of the posterior Arc. Arrows: cFos-ir neurons (black) that coexpressed POMC and mCherry (magenta). Arrowheads: cFos-ir neurons that coexpressed POMC, but no mCherry, **F.** Confocal high magnification image of a cFos-ir neuron coexpressing POMC and mCherry. **G.** Confocal high magnification image of a cFos-ir neuron coexpressing POMC, but not mCherry. **H.** GFP-ir (green) in a Kiss1-hrGFP animal with viral contamination of the posterior Arc. Arrows: cFos-ir (black) neurons that coexpressed Kiss1-hrGFP and mCherry (magenta). **I and J.** Confocal high magnification images of a cFos-ir neuron (arrow in H.) coexpressing Kiss1-hrGFP and mCherry (magenta). Scale bars: 50 µm.

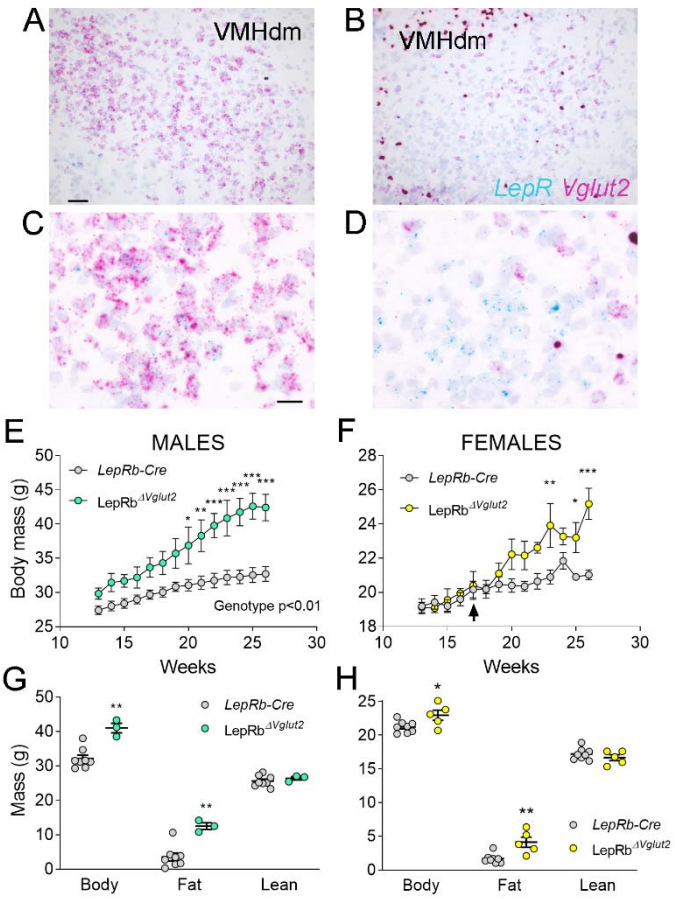

Figure 4. Adult LepRb$^{\Delta Vglut2}$ animals show an obese phenotype. A-D. Micrographs of *in situ* hybridization showing colocalization between *Lepr* (Cyan) and *Vglut2* (Magenta) gene expression in the dorsomedial region of the ventromedial hypothalamic nucleus (VMHdm) in control LepRb-Cre (A, C), but no colocalization in experimental LepRb$^{\Delta Vglut2}$ (B, D) females. A, B. Small magnification, scale bar: 50 µm**.** C, D. Large magnification, scale bar: 20 µm**. E.** Body mass in adult LepRb-Cre and LepRb$^{\Delta Vglut2}$ males (genotype main effect; $F_{1,10} = 13.1$; $p = 0.0047$, post-hoc comparison: week 20: $t_{140} = 3.27$; $p = 0.019$; week 26: $t_{140} = 5.47$; $p < 0.0001$). **F.** Body mass in adult LepRb-Cre and LepRb$^{\Delta Vglut2}$ females (genotype main effect; $F_{1,11} = 4.34$; $p = 0.06$; post-hoc comparisons: week 23: $t_{154} = 4.05$; $p = 0.0011$; week 25: $t_{154} = 3.1$; $p = 0.03$; week 26: $t_{154} = 5.59$; $p < 0.0001$). The arrow indicates the age at which estrus cycling follow-up finished in this cohort. **G.** Body composition in males (fat mass: $t_9 = 3.77$; $p = 0.004$) and **H.** in females (fat mass: ($t_{11} = 3.7$; $p = 0.0035$). *p<0.05, **p<0.01, ***p<0.001.

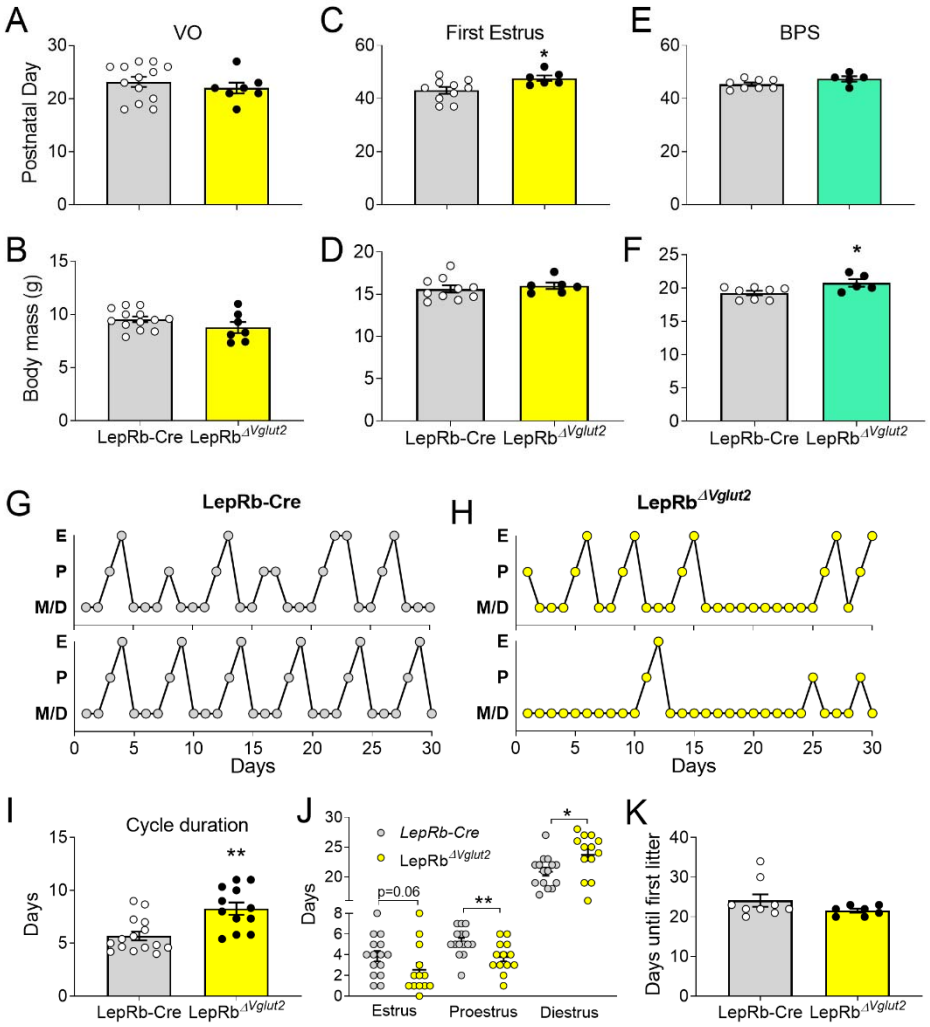

Figure 5. Reproductive development and estrus cycles are altered in LepRb$^{\Delta Vglut2}$ females. **A.** Age of vaginal opening (VO; $t_{18} = 0.84$; $p = 0.41$) and **B.** body mass at vaginal opening (VO) ($t_{18} = 1.47$; $p = 0.16$) in females. **C.** Age of first estrus ($t_{14} = 2.45$; $p = 0.028$) and **D.** body mass at first estrus ($t_{14} = 0.59$; $p = 0.56$) in females. **E.** Age of complete balanopreputial separation (BPS; $t_{11} = 1.80$; $p = 0.1$) and **F.** body mass at BPS ($t_{11} = 2.43$; $p = 0.033$) in males. **G.** Representative estrus cycle profiles from control LepRb-Cre and **H.** experimental LepRb$^{\Delta Vglut2}$ females. (E: estrus, P: Proestrus, M/D: Metestrus/diestrus). **I.** Cycle duration in adult females ($t_{25} = 3.71$; $p = 0.001$). **J.** Time spent in each phase of the cycle during the 30 days studied. Estrus: ($t_{26} = 1.97$; $p = 0.059$), proestrus ($t_{26} = 2.81$; $p = 0.009$), diestrus ($t_{26} = 2.39$; $p = 0.024$). **K.** Days spent from mating until the first litter was observed in females paired with proven male breeders (Mann-Whitney test; $p = 0.32$). *$p<0.05$, **$p<0.01$.

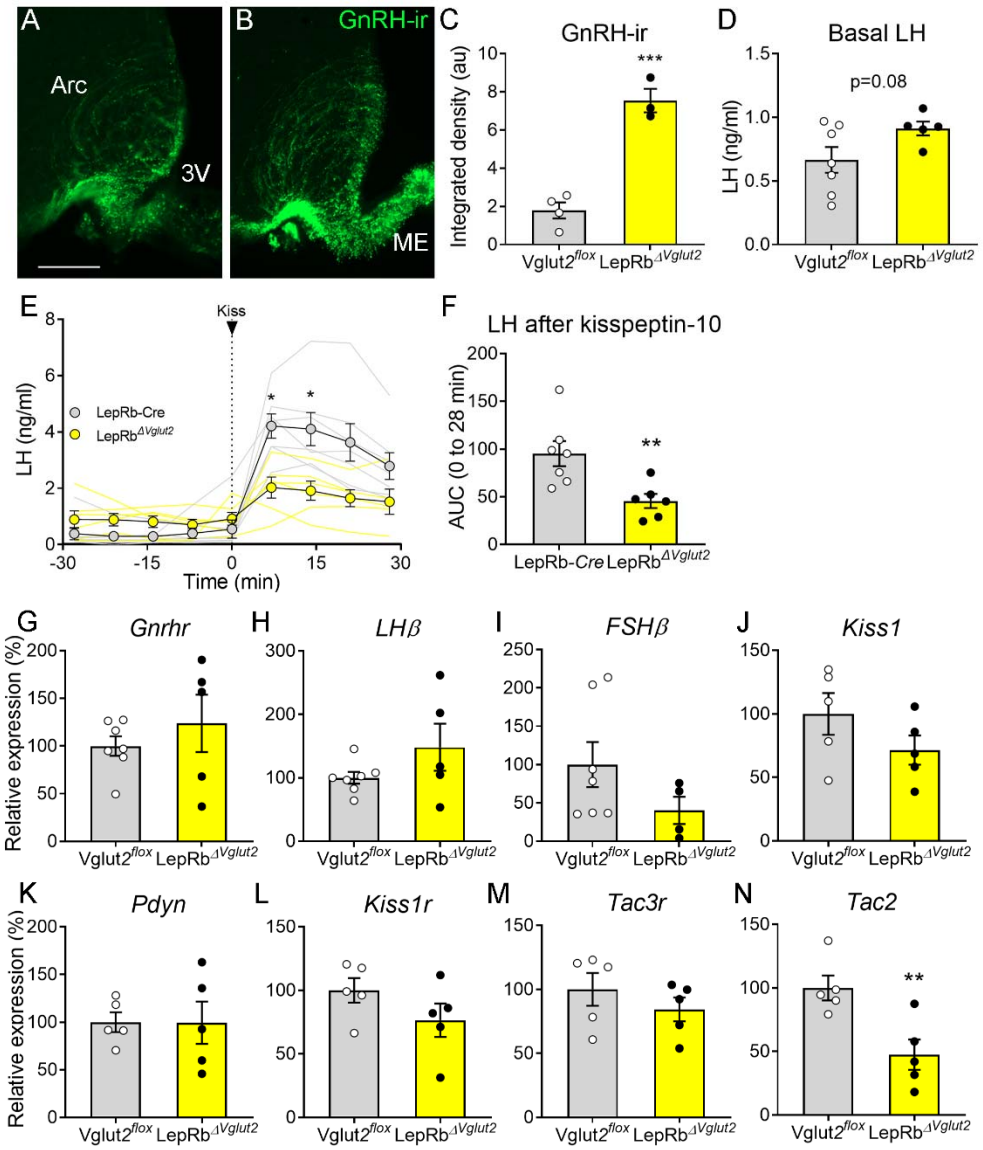

Figure 6. Gonadotropin-releasing hormone (GnRH) content in terminals and luteinizing hormone (LH) secretion are altered in LepRb$^{\Delta Vglut2}$ female mice. Representative fluorescent photomicrograph of GnRH-immunoreactivity (-ir) in the arcuate nucleus (Arc) and median eminence (ME) in **A.** control Vglut2^{flox} and **B.** LepRb$^{\Delta Vglut2}$ diestrous females. Scale bar: 100µm. **C.** GnRH-ir integrated density in the Arc in Vglut2^{flox} (n = 4) and LepRb$^{\Delta Vglut2}$ (n = 3) females (t_5 = 8.01; p = 0.0005). **D.** Basal LH levels in Vglut2^{flox} (n = 7) and LepRb$^{\Delta Vglut2}$ (n = 5) females (t_{10} = 1.91; p = 0.08). **E.** LH levels in LepRb-*Cre* (n = 7) and LepRb$^{\Delta Vglut2}$ (n = 6) females before and after a kisspeptin-10 (65 µ/kg) intraperitoneal (ip.) injection of kisspeptin at time=0. Light grey: individual LepRb-*Cre* females, Light yellow: individual LepRb$^{\Delta Vglut2}$ females. After the injection

(time 7 to 28), LH levels were higher in control than in floxed females (Mixed effects model: main effect for “time” $F_{1.14,\ 12.19} = 15.91$, p=0.001; “genotype" $F_{1,\ 11} = 8.26$, p=0.015; “time x genotype” interaction: $F_{3,\ 32} = 5.00$, p=0.006; Sidak’s post-hoc effect for 7 min ($t_{10.97} = 3.79$, p=0.01) and for 14 min ($t_{9.4} = 3.22$, p=0.04). **F.** Area under the curve (AUC) of LH levels after the kisspeptin injection, ($t_{11} = 3.14$; p = 0.009). **G.** *Gnrhr* ($t_{10} = 0.86$, p = 0.41), **H.** *LHβ* ($t_{10} = 1.47$, p = 0.17) and **I.** *FSHβ* ($t_9 = 1.63$, p = 0.14) relative to Actin B (*Actb*) mRNA levels in the pituitary of Vglut2^{flox} (n = 7) and LepRb$^{\Delta Vglut2}$ (n = 5) females. **J.** *Kiss1* ($t_8 = 1.42$, p = 0.19), **K.** *Pdyn* ($t_8 = 0.02$; p=0.98), **L.** *Kiss1r* ($t_8 = 1.44$, p = 0.19) **M.** *Tac3r* ($t_8 = 0.99$, p = 0.35) and **N.** *Tac2* ($t_8 = 3.39$, p = 0.009), relative to β -2-microglobulin (*B2m*) mRNA levels in the mediobasal hypothalamus of Vglut2^{flox} (n = 5) and LepRb$^{\Delta Vglut2}$ (n = 5) females. *p<0.05; **p<0.01; ***p<0.001.

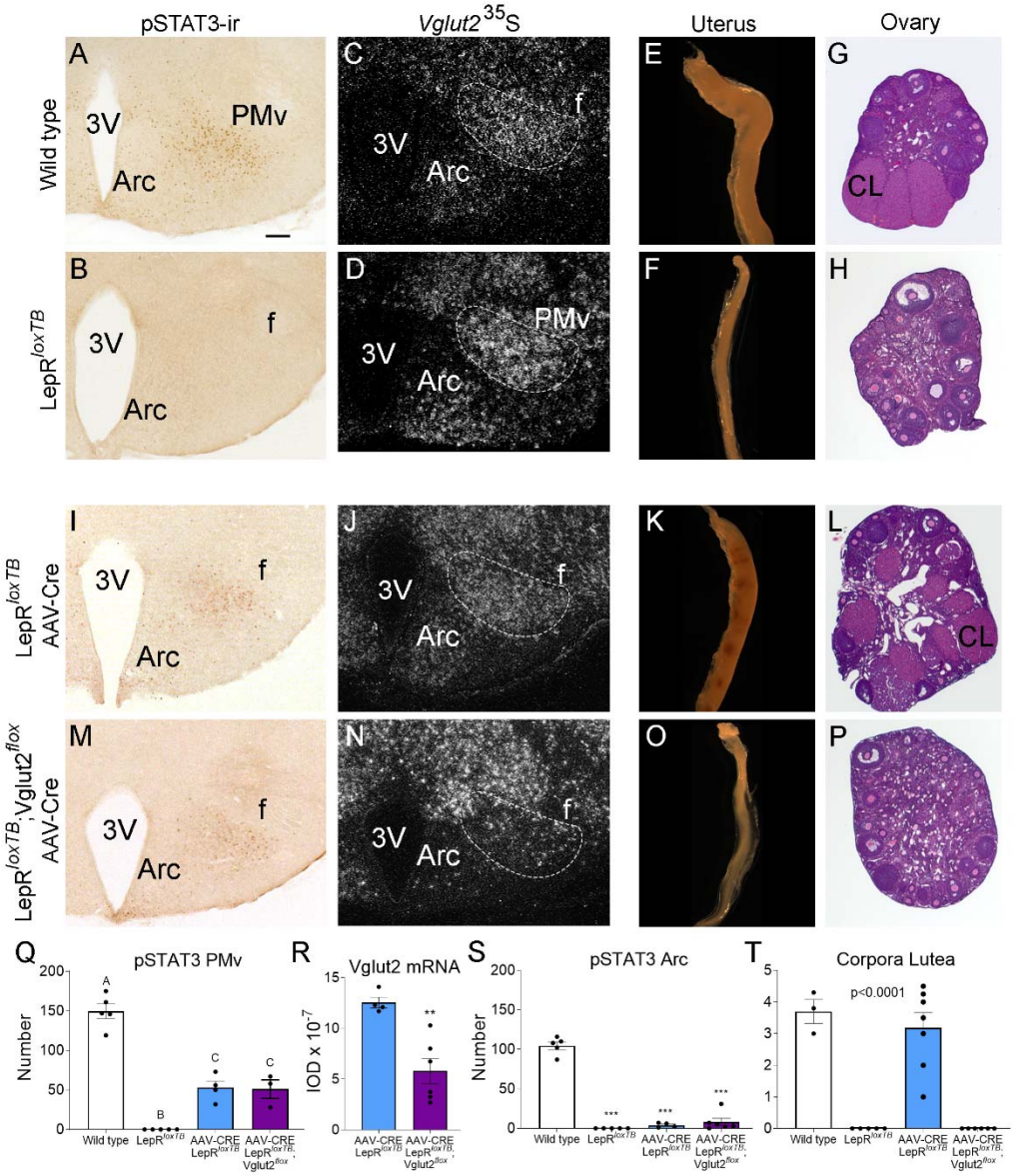

935

936 **Figure 7. Glutamate signaling from the ventral premammillary nucleus (PMv) is required**
937 **for leptin effect on pubertal development in female mouse. A, B, I, M.** Microphotographs of
938 the PMv showing pSTAT3-ir following leptin administration. Note lack of pSTAT3-ir in
939 LepR^{loxTB} mouse. **C, D, J, N.** Darkfield microphotographs showing *Vglut2* mRNA (silver grains)
940 in the PMv. Note decreased *Vglut2* mRNA expression in LepR^{loxTB};Vglut2^{flox} mice injected with
941 AAV-Cre. **E, F, K, O.** Microphotographs of representative single uterine horns. Note lack of
942 uterine growth in LepR^{loxTB} mouse and in LepR^{loxTB};Vglut2^{flox} mouse injected with AAV-Cre. **G,**
943 **H, L, P.** Microphotographs of representative ovary sections. Note lack of *corpora lutea* in
944 LepR^{loxTB} mouse and in LepR^{loxTB};Vglut2^{floxed} mouse injected with AAV-Cre. 3V: Third

ventricle, Arc: Arcuate nucleus, f: fornix, CL: *Corpus luteum.* Scale bars: 100µm. **Q.** Number of pSTAT3 expressing cells in the PMv in Wild-type (n=5), LepR^{loxTB} (n=5), AAV-CRE injected LepR^{loxTB} (n=4), and AAV-CRE injected LepR^{loxTB};Vglut2^{flox} (n=3) ($F_{3,13}$= 73.53, p<0.0001). **R.** Quantification of the *Vglut2* hybridization signal in the PMv AAV-CRE injected LepR^{loxTB} (n=4), and AAV-CRE injected LepR^{loxTB};Vglut2^{flox} (n=6) (t_8 = 4.20; p = 0.003). **S.** Number of pSTAT3 expressing cells in the Arc ($F_{3,16}$= 171.8, p<0.0001). **T.** Number of corpora lutea in the ovary ($F_{3,17}$= 31.16, p<0.0001).

Table 1. Experimental groups in the study of chemogenetic activation of LepRb-Cre cells in the PMv. Corresponding to figures 1-3. The number of animals in each group is indicated in brackets.

AAV Vector	Drug	Injection site	LH increase 10-20 min	Group name	Color in Figs 1E-H, 2 and 3
AAV-hM3Dq (18)	CNO	Hit in PMv (15)	Yes (8)	"PMv-Hit" with LH increase	
			No (7)	"PMv-Hit" with no LH increase	
		Missed PMv (2)	No	Negative controls	
		No cFos in mCherry cells. Removed from analysis (1).			
AAV-mCherry (5)	CNO	Hit in PMv	No	Negative controls	
AAV-hM3Dq (4)	Clozapine	Hit in PMv	Yes	Clozapine hM3Dq	
No AAV (7)	Clozapine	No injection	(2/7)	Clozapine no AAV	

Table 2. Antibodies

Antibody	Protein target	Host organism	Dilution used	Vendor and cat#	RRID
Anti-GFP (Chicken Antibodies, IgY Fraction)	recombinant GFP null	Chicken	1:10000	Aves Labs Cat# GFP-1010	AB_2307313
mCherry monoclonal (16D7)	mCherry tag	Rat	1:5000	Thermo Fisher Scientific Cat# M11217	AB_2536611
ABE457 | Anti-cFos	N-terminus	Rabbit	1:2000	Millipore	AB_2631318

	cFos			Cat# ABE457	
Pro-opiomelanocortin Precursor POMC (27-52) antibody	Aminoacids 27-52 of porcine POMC peptide null	Rabbit	1:10000	Phoenix Pharmaceuticals Cat# H-029-30,	AB_2307442
Anti LHRH (GnRH)	Synthetic LHRH	Rabbit	1:1000	Immunostar Cat# 20075	AB_572248
Phospho-Stat-3 (tyr705)	Phospho-Stat-3 (tyr705)	Rabbit	1:1000	Cell Signaling Technology Cat# 9131	AB_331586
Goat anti-Chicken IgY, Alexa Fluor 488	Chicken, IgY (H+L)	Goat	1:500	Thermo Fisher Scientific Cat# A-11039	AB_2534096
Donkey anti-Rat IgG, AlexaFluor 594	Rat IgG (H+L)	Donkey	1:500	Thermo Fisher Scientific Cat# A-21209	AB_2535795
Donkey anti-Rabbit IgG, AlexaFluor 488	Rabbit IgG (H+L)	Donkey	1:500	Thermo Fisher Scientific Cat# A-21206,	AB_2535792
Biotin-SP-conjugated AffiniPure Donkey Anti-Rabbit IgG	Rabbit IgG (H+L)	Donkey	1:1000	Jackson ImmunoResearch Labs Cat# 711-065-152	AB_2340593

957

Table 3. Quantitative PCR primers

Gene	Primer Sequence	NCBI accession N.	Vendor
Actb	Fwd 5'-GGCTGTATTCCCCTCCATCG-3' Rev 5'-CCAGTTGGTAACAATGCCATGT-3'	NM_007393.5	IDT
B2m	Fwd 5'-TCTCACTGACCGGCCTGTAT-3' Rev 5'-GATCACATGTCTCGATCCCAGT-3'	NM_009735.3	IDT
CGA	Fwd 5'-CCTCAGATCGACAATCACCTG-3' Rev 5'-AGCATGACCAGAATGACAGC-3'	NM_009889.2	IDT
FSHβ	Fwd 5'- CTGGTGCTGGAGAGCAATCT -3' Rev 5'- ACTTTCTGGGTATTGGGCCG -3'	NM_008045.3	IDT
Kiss1	Fwd 5'-GGCAAAAGTGAAGCCTGGAT-3' Rev 5'-GATTCCTTTTCCCAGGCATT-3'	NM_178260.4	MWG|operon
Kiss1r	Fwd 5'-TGGCTGGTTCCCCTGTTTTT -3' Rev 5'-GCAGCCAGGTTAGCGATGTA -3'	NM_053244.5	IDT

GnRH1	Fwd 5'-GGGAAAGAGAAACACTGAACAC-3' Rev 5'-AGTACATTCGAAGTGCTGGG-3'	NM_008145.4	IDT
GnRH-r	Fwd 5'-TCTTCATCATCCCCCTCCTC-3' Rev 5'-GGAGTCCAGCAGACGACAAA -3'	NM_010323.2	IDT
LHβ	Fwd 5'- CCAGTCTGCATCACCTTCAC -3' Rev 5'- CAGCTGAGGGCTACAGGAAAG -3'	NM_008497.2	IDT
Pdyn	Fwd 5'-CGTTGCTGTCAAGATCTGTTG -3' Rev 5'-AGGCAGTCCGCCATAACATT -3'	NM_001286502.1	IDT
Tac2	Fwd 5'-TCTGTGTGGGATGTAAAGGAGGG-3' Rev 5'-GACAGCCGCAAACAGCATGG-3'	NM_001199971.1	IDT
Tac3r	Fwd 5'-TAAAAGTCATGCCAGGCCGT -3' Rev 5'-AGGTGACACCCATGATGAGC -3'	NM_021382.6	IDT

958